



UNIVERSITY OF CALIFORNIA, SAN DIEGO

Design Report

Furious Flier

March 11, 2003

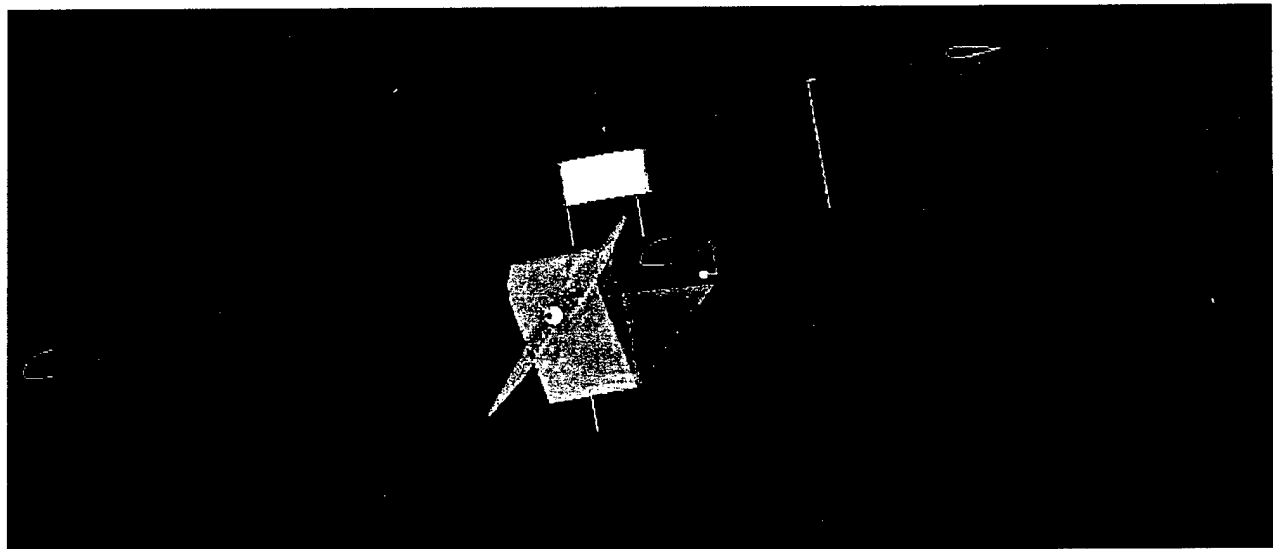


Table of Content

1.0 Executive Summary	4
1.1 Objective	4
1.2 Analytical Tools	4
1.3 Conceptual Design Phase	5
1.3.1 Goals	5
1.3.2 Methodology	5
1.4 Preliminary Design Phase	5
1.4.1 Goals	5
1.4.2 Methodology	6
1.5 Detailed Design Phase	6
2.0 Management Summary	7
2.1 Team Personnel	7
2.2 Sub-team Responsibilities	7
2.2.1 Propulsion	8
2.2.2 Structure	8
2.2.3 Aerodynamics	8
2.2.4 Stability/Controls	8
2.2.5 Performance	8
2.2.6 Construction	8
2.2.5 Task Scheduling	9
3.0 Conceptual Design	11
3.1 Design Parameters	11
3.1.1 Main Design Parameters	11
3.1.2 Rated Aircraft Cost	11
3.2 Aircraft Configuration	11
3.2.1 Fuselage and Tail Configuration	11
3.2.2 Wing Configuration	12
3.2.3 Landing Gear Configuration	13
3.2.4 Selecting a Payload Deployment System	14
3.3 Determining the Power Plant Configuration	15
4.0 Preliminary Design Phase	17
4.1 Determining the Optimum Number of Batteries	17
4.2 Motor Selection	18
4.3 Trade Study of Planform Area	19
4.4 Optimizing Tail Sizing	21
4.5 Payload Deployment System	21
4.6 Spar Analysis and Optimization	23
5.0 Detailed Design	25
5.1 Summary of Aircraft Geometry and Features	25
5.1.1 Fuselage Features	26
5.1.2 Wing Features	27
5.1.3 Tail Features	27
5.2 Assessing the Airfoil Properties	27
5.3 Properties o the Propulsion System	33
5.4 Static Stability	34
5.5 Mission Performance	36
5.6 Rated Aircraft Cost	38
5.7 Drawing	39
5.7.1 Overall Aircraft Design	39
5.7.2 Fuselage Structure with Payload Deployment System	40
5.7.3 Dimension of the Wing Assembly	41

5.7.4 Dimension of the Tail	42
6.0 Manufacturing Plan and Techniques for Furious Flier	43
6.1 Manufacturing Processes and Feasibility	43
6.2 Manufacturing Processes by Aircraft Component	43
6.2.1 Manufacturing FF's Wings and Empennage	43
6.2.2 The Spar and Spar Joiner Construction	44
6.2.3 Fuselage Construction	45
6.2.4 Boom	46
6.2.5 Landing Gear Manufacturing	46
6.3 Costs, Skills, and Schedules	46
6.3.1 Costs of Composites Materials	46
6.3.2 Skills and Tools Needed to Work with Composites	46
6.3.3 Manufacturing Schedule	46
7.0 Test Plan	48
7.1 Dynamic Testing: Graupner Motor	48
8.0 Work Cited	50

Table of Figures

Figure 2.1: Milestone Chart	10
Figure 3.1: Conceptual Design Considerations for the Payload Deployment Mechanism ..	14
Figure 3.2: Motor Configuration	16
Figure 4.1: Plot of the Number of Cells vs. Predicted Score	18
Figure 4.2: Planform Area vs. Predicted Score	19
Figure 4.3: Aspect Ratio vs. Predicted Score	20
Figure 4.4: The Payload Deployment System	22
Figure 4.5: Cross Section of the Spar	24
Figure 5.1: Coefficient of Lift C_L vs. Angle of Attack AOA	29
Figure 5.2: Coefficient of Lift C_L at Cruise Speed vs. Angle of Attack AOA	29
Figure 5.3: Coefficient of Pitching Moment at the Quarter Chord vs. Angle of Attack AOA ..	30
Figure 5.4: Lift to Drag Ratio vs. Angle of Attack AOA	31
Figure 5.5: Lift to Drag Ratio for Various Airfoils	31
Figure 5.6: Center Pressure vs. Angle of Attack	32
Figure 5.7: Angle of Climb Diagram	36
Figure 5.8: Rated Aircraft Cost	37
Figure 6.1: Gantt Chart	43
Figure 7.1: Dynamometer Plot	48

Table of Tables

Table 2.1: Structure of the Team	7
Table 3.1: Decision matrix of the payload deployment system	14
Table 3.2: Decision Matrix of the Motor Configuration	16
Table 4.4: Deployment Mechanisms Considered and Tested	22
Table 4.5: Relevant Dimensions to Estimate the Bending Moment	23
Table 5.1: Fuselage Sizing	25
Table 5.2: Wing Sizing with a S4022 Airfoil	26
Table 5.3: Empenage Sizing with a S9027 Airfoil	26
Table 5.4: Weight Estimation of Aircraft Parts	33
Table 5.5: Center of Gravity	34
Table 5.6: Predicted Performance of the Aircraft	36
Table 5.7: Estimated Rate of Climb Performance	37
Table 5.8: Rated Aircraft Cost	38

1.0 Executive Summary

This report summarizes what the student members of the American Institute of Aeronautics and Astronautics (AIAA) at the University of California, San Diego carried out in order to fulfill the objectives for the 2002/2003 AIAA Design/Build/Fly Competition.

The AIAA Design/Build/Fly (DBF) Competition emphasizes the importance of design, construction, and the actual flight performance of the final plane. Based on one of the Mission Tasks requiring the aircraft to self-deploy a simulated sensor package, the team designed the aircraft to carry a payload with the dimensions of 6 inches wide by 6 inches tall by 12 inches long and weighing at least 5 lbs., with a take-off distance less than 120 ft. The wingspan is approximately 7ft. in length, and the empty weight is 13.5 lbs. The final score given to the design is based upon a Written Report Score, Total Flight Score and the Rated Aircraft Cost.

1.1 Objectives

The objective of the contest is to design, fabricate, and demonstrate the flight capability of an unmanned, electric powered, radio controlled aircraft dubbed the "Furious Flier" to meet the best two of three required missions specified in the rules: Missile Decoy, Sensor Deployment, or Communications Repeater. The electric powered aircraft must possess good handling characteristics and has exceptional performance, while remaining practical and affordable to manufacture. The lowest RAC and the highest flight score were achieved through trade studies, comparing the properties of different motors, number of batteries, and the aerodynamic properties of various airfoils.

1.2 Analytical Tools

Several analytical tools were used throughout the entire design process. The most important was Microsoft Excel, which was used for estimating the flight conditions, flight performance, propulsion properties, and Rated Aircraft Cost. Visual Foil 3.0 allowed the team to analyze the aerodynamic properties of various airfoils under different flight speeds. The Electric Motor Calculator allowed the team to compare motors, propeller span and pitch, and battery cell configurations. The wind tunnel allowed the team to compare a scaled-down version of the team's selected airfoil, which is the Selig S4022, with the theoretical aerodynamics properties of the airfoil. Finally, the programs AutoCAD 2000 and PRO/ENGINEER 2001 were important tools to visualize and create two dimensional or three dimensional models.

1.3 Conceptual Design Phase

1.3.1 Goals

The operative goal for the Conceptual Design Phase (CDP) was to create a basic “outline” for the airplane. By the end of the phase, we intended to have a basic silhouette of the airplane showing its basic shape and configuration. This stage was dedicated to placing and fixing basic body, wing, and tail details. In order to determine a basic configuration for the aircraft, the team would also have to determine which of the three missions aircraft would perform.

1.3.2 Methodology

Before a task-specific airplane can be designed, its tasks must first be assigned. The team was divided up into three different groups, with each group being assigned a mission and given the responsibility for fully analyzing it and drawing up a list of pros and cons. The results were then input into a decision matrix or Figure of Merit (FOM) to determine which combination of missions would present the most empirical benefit. Utilizing the decision matrices, team members voted to pick the final conceptual design of the aircraft and the combination of missions to perform.

Each team member came up with several designs which they felt best met the mission goals while providing speed, stability, and the lowest Rated Aircraft Cost (RAC). The designs were presented and then evaluated for ideas and innovations. The designs were broken down into their key components: wing position, tail type, engine placement, basic body shape, and deployment mechanism. Variations for each design element were then analyzed and their merits were weighed till an ultimate winner in each category was established. Each of the elements was then pieced together into a final design. In terms of wing positioning, three different setups were evaluated: a low wing, high wing, and a canard system. Four separate tail setups were also considered, ranging from the traditional layout, to a T-Tail, V-Tail, as well as an H-Tail. Two different engine placements were also evaluated: a conventional puller configuration and a pusher. Six different fuselage types were evaluated, encapsulating three different drop mechanisms. Primary plane characteristics, such as body type, engine placement, and payload deployment system were evaluated for their strength, ease of construction, contribution to a low RAC and ease of combination with secondary plane characteristics such as wing location and tail type. Emphasis was placed on developing the most efficient and aerodynamic, yet simplest, structure possible.

1.4 Preliminary Design Phase

1.4.1 Goals

The purpose of the Preliminary Design Phase was to perform trade studies and optimizations analysis on the aircraft to achieve the highest flight score possible and the lowest RAC possible. Once the Conceptual Design Phase was complete, the properties of competing component configurations of

the aircraft were assessed in the Preliminary Design Phase. The best configurations were selected out of the competing the configurations.

1.4.2 Methodology

To optimize the aircraft, each sub-team performed analysis on components of the aircraft. The Aerodynamics sub-team used Visual Foil 3.0 to compare three competing airfoils before selecting the Selig S4022 airfoil that would provide the best lift under 120 feet. Alternative airfoils that were considered were Eppler E214 and the Selig S3002. They also analyzed the planform area that would give the lowest RAC while also providing the best flight performance score. The Propulsion sub-team used Motor Calculator to compare different motors, their efficiencies and the battery counts in selecting the motor that would give the best performance under the given constraints of having a 40A fuse. The motor selected was the Graupner 3300/5 over the Graupner 3300/6 and the Graupner 3300/7. The Structures sub-team analyzed the load on the wing joiner and optimized the spar to determine whether the component would fail under loads.

1.5 Detailed Design Phase

The Detailed Design Phase was less focused on actual aircraft configuration design as compared to the previous two phases. The focus in this section was to provide estimated performance, sizing, aerodynamics, and stability properties of the aircraft. The sub-teams worked to finalize the design of the aircraft in the Detailed Design Phase. The Propulsion sub-team finalized the power plant configuration, selecting the motor, the propeller span and pitch, and the battery configurations to be used. The Aerodynamics sub-team selected the airfoil after analyzing properties such as the pitching moment coefficient, the coefficient of drag, and the coefficient of lift, investigating the aerodynamics properties of the airfoil under different airspeeds. The Stability/Controls sub-team provided the estimated weight and the center of gravity of the aircraft through analyzing each component of the aircraft. The Structures sub-team provided the Drawing Packages and dimensions of the various components of the aircraft. The Performance sub-team provided the estimated turning radius, range, rate of climb, and cruise speed of the aircraft.

2.0 Management Summary

2.1 Team Personnel

The UCSD Furious Flier team is composed of five sub-teams where the team members ranged from Seniors to Freshmen and one project manager. The six sub-teams were Aerodynamics, Structures, Propulsion, Stability/Controls, Propulsion, and Construction. In every sub-team, one lead engineer is responsible for determining the overall direction of the sub-team and providing the individual members within the sub-teams proper tools and references to solve problems pertaining to the design of the Furious Flyer aircraft. Each member was not restricted to his sub-team as knowledge and expertise was shared within the various groups. The Construction sub-team had a lead engineer student but all members were able to contribute to the construction of the plane. It should be noted that most of the members on the Furious Flyer team have never competed in AIAA/ONR Design/Build/Fly and are learning from phases of construction. The criteria to be a lead engineer student in a sub-team were that the member must be a Junior or Senior who have taken the necessary courses pertaining to either Aerodynamics, Structures, Stability/Control, Propulsion, or Construction, and mentor underclassmen in the field that they are responsible for. Below is Table 2.1, showing the members within each sub-team and the lead engineer student in charge of the sub-team.

Table 2.1: Structure of the Team

Aerodynamics	Structures	Propulsion	Performance	Stability	Construction
Lead: Dana Pugh	Lead: Dan Dalton	Lead: Mann Chau	Lead: Patty Martinez	Lead: Andrew Fischer	Lead: Chad Valenzuela
Wings: Jeremy Bank	Fuselage/landing: Freddy Torrez Wendy Peterson Vladimir Guzaev	Current Analysis: Jeremy Bank	Predicted Performance: Jeremy Bank	Center grav.: Jeremy Bank	Wendy Peterson Mann Chau Vladimir Guzaev Brooke Mosely
Tail Sizing: Andrew Fischer	Payload: Amit Mulgonkar		RAC: Brooke Mosely		Freddy Torrez Amit Mulgonkar

2.2 Sub-team Responsibilities

The overall configuration of the aircraft was the combination of the design contribution of every sub-team members. Components were designed such that members collaborated about possible configurations. Often when collaborating among the lead engineers, compromises were made to fit the components together within the limited space.

2.2.1 Propulsion

The purpose of the Propulsion sub-team was to evaluate the properties of batteries, propellers, and motors on the overall thrust of the aircraft and Rated Aircraft Cost (RAC). The Propulsion sub-team was responsible for deciding on whether to configure the aircraft as a pusher or puller. Analysis was performed using the Electric Motor Calculator software to determine theoretical properties of different Graupner series motors.

2.2.2 Structures

The Structures team designed and analyzed the properties of the fuselage, landing gears, payload deployment system, skin, and tail under loads based on the mission requirements of the competition. The Structures team analyzed the optimum spar cross section configuration and determined the points at which the aircraft is most likely to fail. Among the tools used was Pro-Engineer, Pro-Mechanica, and AutoCAD.

2.2.3 Aerodynamics

Each member of the Aerodynamic group observed the use of Visual Foil software. From the results of the chosen airfoil, the coefficient of lift, the coefficient of drag, and the coefficient of the pitching moment at the quarter chord was collected for three different velocities. Each member was given a task in analyzing and understanding the data. The maximum coefficient of lift, the maximum lift to drag ratio, and finite wing analysis were the main calculations determined from the data.

2.2.4 Stability/Controls

The Stability and Controls sub-team assessed the center of gravity, center of lift, pitching moment and provided the tail sizing of the aircraft based on those properties. They collaborated with the Performance and Aerodynamics sub-team to optimize flight stability properties and handling of the aircraft.

2.2.5 Performance

The Performance sub-team assessed the flight characteristics of the aircraft. They were responsible for assessing the flight conditions during the competition, cruise speed, stall speed, take-off distance, rate of climb, turning radius and range. The Performance sub-team also collaborated with the Stability/Controls and Aerodynamics sub-team to assess the performance of the aircraft under various flight conditions.

2.2.6 Construction

The purpose of the Construction team was, simply put, to build a low weight, high strength, and high quality aircraft to submit into this year's Design/Build/Fly competition. It is their duty to ensure that component parts for the fuselage, empennage, and landing gear are made with precision and pride. Manufacturing was a team effort from the first brainstorm of a conceptual design, to placing the last

sponsor's sticker on the wing. Manufacturing an airplane takes time, patience and dedication. This team came together to exemplify that notion and has built a very strong plane.

2.2.5 Task Scheduling

In early November, the group decided upon a schedule of completion dates. Each subgroup was expected to complete tasks by a certain deadline. The chart below (Figure 2.1) depicts the milestones and actual dates of completion of each major event. Problems that were encountered completing these tasks were quickly resolved through teamwork and subgroup collaboration.

Figure 2.1: Milestone Chart

Mile Stone	6-Jan	13-Jan	20-Jan	27-Jan	3-Feb	10-Feb	17-Feb	24-Feb	3-Mar	10-Mar	17-Mar	24-Mar	31-Mar	7-Apr	14-Apr	21-Apr
Finalize Preliminary Design																
Prepare for Professional Design Review (PDR)																
PDR (Jan 23, 2003)																
Construct Wings (Foam Core to Layup)																
Construct Foam Core Spar and Test																
Construct Payload and Deployment System																
Construct Antenna and Mounts																
Construct Balsa Wood Core Spar and Test																
Construct Fuselage (Composite Panels)																
Construct Empennage (Foam Cores to Layup)																
Assemble Empennage Connection to Boom																
Written Report																
Construct Landing Gear and Hard Points																
Construct Nosecone and Motor Mounts																
Complete All Electrical Circuitry																
Finalize All Construction																
Test Flights																
Competition																
Projected																

3.0 Conceptual Design

To first start the conceptual design process, the requirements for each mission were determined. Next, concepts for the aircraft were decided as to meet the requirements. Each design concept was thoroughly discussed and critiqued, and then the best aspects of each concept were found and compiled into one design. This concept was the basis for our final design.

3.1 Design Parameters

A design strategy was formulated based on the requirements of the aircraft during the mission.

3.1.1 Main Design Parameters

Certain specifications were deemed more important than others in order to maximize the point total in our aircraft development. Weight of the aircraft, number of engines, lift and drag of the wings, and wing sizing were the main factors we looked at to affect the aircraft.

Being able to take off in the allotted space was a major concern. In all of the initial calculations, the takeoff distance was too long for what was required. The sizing, lift, and drag of the wing reflected the need to take off in a short distance. Maximizing the performance of each did this.

The number of engines was lowered in order to lower the RAC of the aircraft, but this lessened the power of the aircraft, which limited its performance, but the reduced RAC outweighed the worse performance.

3.1.2 Rated Aircraft Cost

The RAC of the aircraft was a major factor in the design of the aircraft. Limits in aircraft design were created in order to minimize the RAC, while not limiting the aircraft to a point where it could not be made effectively. The RAC is based mainly on weight, battery weight, number of engines, fuselage size, wing sizing, control surfaces and servos. The weight of the batteries, the weight of the aircraft, and the number of engines are very large factors in the RAC. Knowing this, the weight and engines were reduced.

3.2 Aircraft Configuration

Once the initial specifications were decided, each aspect of the actual aircraft was looked at. Figures of Merit were used to rate each possibility for every aspect of the aircraft.

3.2.1 Fuselage and Tail Configuration

Figures of Merit were used to analyze the effect of the RAC, size specifications, performance, and handling of the aircraft on the fuselage and tail design. These analyzed figures of merit were used in

accordance with the design specifications created to decide upon the most effective and realistic alternatives for the fuselage and tail.

In regard to the fuselage, the main two alternatives were a flying wing, or a conventional body type. Based on the dimensions required to hold the payload, a flying wing type body was decided to be incompatible. This was because the body structure for the flying wing would have to be too large to fit the payload.

The tail however, took more analysis. A conventional tail, a V-tail, a H-Tail, and a T-tail were all considered. A conventional tail is fairly good all around, except the fact that disturbances from the body and antenna could affect the handling of the aircraft during flight. A V-tail would have a better RAC than the others because of fewer surfaces, but other than that, would be fairly similar. An H-tail, would reduce the effects of disturbances on the tail and increase handling, but would increase the RAC because of more control surfaces. A T-tail allows the horizontal stabilizers to clear the disturbances of the fuselage and antenna, while keeping the RAC relatively low. After rating each configuration concept, it was decided that the T-tail would suit the requirements the best, so it was chosen.

Fitting the boom of the tail inside the size constraints was a major concern, so it required a lot of decisions and analysis. To fit the boom inside the box, it had to move from its position for flight while inside the box. Possibilities were: a folding boom, a detachable boom, or a sliding boom. A folding boom would lessen the stability and strength of the boom, but would allow it to fit inside the box. A detachable boom would fix the size constrain problem, but adds to the assembly time. A sliding boom could create a problem with slight movements in flight. The strength of the boom was deemed an important aspect, as was the fact that slight movements in the tail create handling difficulty. These factors caused the decision for a detachable boom, even at the cost of an increased assembly time.

3.2.2 Wing Configuration

Payload deployment, flight stability, and construction all were analyzed figures of merit for the wing configuration.

- Deployment of the payload had a very large effect on the wing design because only certain deployment mechanisms would work for certain wing designs.
- The placement of the wings can create very stable or very unstable flight conditions.
- Certain wing types are more easily created than others; this must be taken into account because of time and material limitations.

There are three types of wing design possibilities that were compared: low, middle, and high wing designs.

- **Low Wing**: A low wing design provides a little less stability, but requires less structural support than other wing possibilities. It also creates problems in deploying the payload, forcing it to come out behind the aircraft, instead of below it.
- **Middle Wing**: A middle wing design is much harder to build than the other configurations and does not allow enough room for the payload to be attached to the aircraft in an efficient manner. It provides structural stability, and some flight stability.
- **High Wing**: A high wing design allows an easy way to deploy the payload, creates stability for flight and is relatively easy to build.

The high wing provides results that can meet the requirements for a wing design by ease of construction, stability, and proper payload deployment methods.

3.2.3 Landing Gear Configuration

The structural strength, payload clearance, drag, and weight were the figures of merit analyzed for the landing gear configuration.

- The structural strength of the landing gear is a very important factor because the landing gear must be strong enough to support the weight of the aircraft while landing.
- The landing gear must also be big enough to clear the payload while on the aircraft and when it is deployed.
- The amount of drag of the landing gear can affect the flight of the aircraft, so should be minimized.
- The weight of the landing gear is a major factor because more weight adds to our RAC, so any weight we can cut down on landing gear is very helpful.

The three types of landing gear considered were a tricycle, a quadacycle, and a tail-dragger. Having a continuous piece to support the landing gear creates a stronger support and increases its structural strength, so it was an advantageous design to use. It is assumed that each design could be made to clear the payload, and have a continuous piece for support of the landing gear.

- A tricycle design for the landing gear could reduce the weight and drag from the quadacycle because of a three-wheel design, instead of a four-wheel design.
- A quadacycle design creates a more stable wheelbase, but can create more weight and drag because of an extra wheel.

- A tail-dragger design has three wheels, as does the tricycle, but becomes unstable as wind conditions get high.

The tricycle design was not quite as stable as the quadacycle design, but the reduced weight and drag make it a better design for the requirements.

3.2.4 Selecting a Payload Deployment System

The Sensor Deployment mission requires that the aircraft fly two laps, land, release a 6"x6"x12" payload, and fly two more laps. Several conceptual design configurations were considered. In Figure 3.1, four design configurations were considered for the payload deployment systems. In System A, a solenoid pushes the payload from out of the fuselage; in System B, a servo pulls a trigger mechanism that would release the payload down; in System C, a motor pulls the belly of the fuselage open for the payload to drop; and in System D, a servo pulls a pin from a tab, which is a permanent part of the payload, causing the payload to drop directly down.

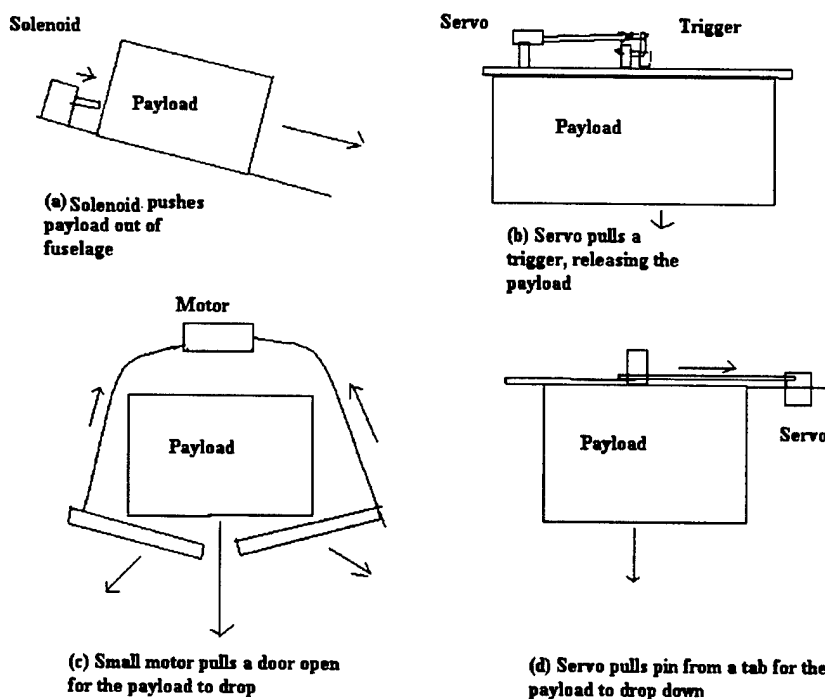


Figure 3.1: Conceptual design considerations for the payload deployment mechanism

The deployment mechanism designs were weighed against each other based on the ease of manufacturing, RAC concerns, and reliability. The mechanism itself must function with little or no technical difficulties, so reliability was given the most weight. Manufacturing the payload deployment

system could be a potential problem, so it was also weighed in. Because all of the deployment mechanisms require an extra servo, motor, or solenoid and because these devices add weight, the RAC concerns was also factored into the decision process. Below is a Figure of Merit study between the four competing designs (Table 3.1).

Table 3.1: Decision matrix of the payload deployment system.

Figures of Merit	Reliability (x50)	RAC (x30)	Ease of Manufacturing (x20)	Total Score	Decision
A	-1	-1	1	-30	Rejected
B	0	0	-1	-20	Rejected
C	-1	-1	-1	-100	Rejected
D	1	0	1	70	Kept

Based on weighing the concerns of the reliability, RAC score, and the ease of manufacturing, System D was chosen.

3.3 Determining the Power Plant Configuration

Several design configurations of the motors and batteries were considered. In Figure 3.2, three main design configurations of the propulsion systems were considered: (a) one motor with 18 nickel-cadmium cells, (b) two motors with 9 cells each, and (c) two motors connected in series to a total of 18 cells. When considering each configuration, the RAC was given the most weight, followed by the power, weight, and efficiency. Below is a Figure of Merit decision matrix between these options (Table 3.2).

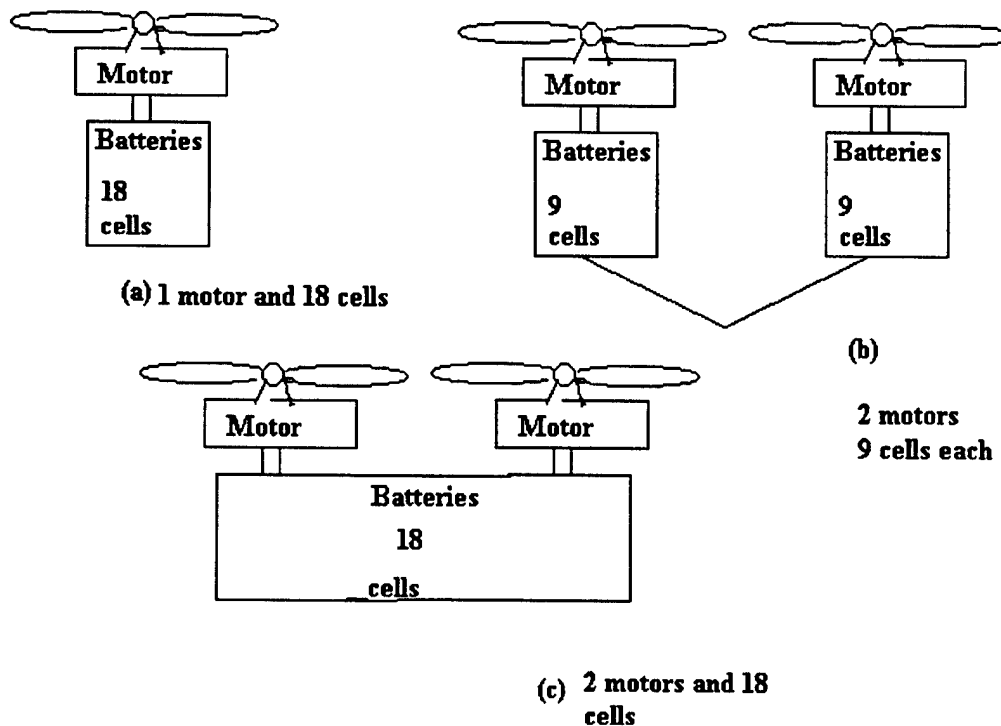


Figure 3.2: Motor configurations

Table 3.2: Decision Matrix of the Motor Configuration

Figures of Merit	RAC (x30)	Efficiency (x20)	Power (x25)	Weight (x25)	Total Score	Decision
1 motor 18 cells	1	1	0	1	80	Kept
2 motors 9 cells each	0	0	1	0	25	Rejected
2 motors 18 cells total	0	-1	1	0	5	Rejected

The final decision was with one motor with 18 cells. The RAC had the greatest weight because while it would be beneficial to have powerful thrust with two motors, having two motors would not be efficient while incurring unnecessary RAC cost, which makes the option less desirable. The three missions can be performed using just one motor with 18 cells. Anything that can be done to reduce RAC and raise efficiency is much more desirable.

4.0 Preliminary Design Phase

The preliminary design phase is a time to perform trade studies, calculate the best flight score results and ultimately optimize the performance of the aircraft based on the final conceptual design. For example, the characteristics of the airfoil were investigated, the tail sizing was selected, and the properties of motors were analyzed for their efficiencies.

4.1 Determining the Optimum Number of Batteries

Analysis was conducted on the number of batteries to be used in flight versus the Total Flight Score. Note that the Single Flight Score is proportional to the Difficulty Factor and inversely proportional to the Mission Flight time while the overall score is proportional to the Total Flight Score and inversely proportional to Rated Aircraft Cost (Eq. 4.1 - 4.2).

$$\text{Single_Flight_Score} = \frac{\text{Difficulty_Factor}}{(\text{Mission_Flight_Time} + \text{Aircraft_Assembly_Time})} \quad (4.1)$$

$$\text{Total_Flight_Score} = \frac{\text{Report_Score} * \text{Flight_Score}}{\text{Rated_Aircraft_Cost}} \quad (4.2)$$

To find the predicted best number of batteries to produce the greatest overall score, certain assumptions had to be made. It was estimated that the Written Report Score would be roughly 85, the Aircraft Assembly Time approximately 1 min and 30 sec, and that the Difficulty Factor would level the performance gaps for each mission. The Electric Motor Calculator software was used to analyze the predicted pitch speed on a Graupner 3300/5 motor under several different numbers of batteries. The number of batteries considered was between 15 and 20 cells. These minimum and maximum cell counts were determined by the very minimum amp hours we could complete the course in and the maximum number of cells the motor could deplete if it were to be run at full power through the entire course. While having large quantities of batteries can provide extended full power to the motors, the weight of the batteries can severely reduce the aircraft's performance by adding substantial weight and by increasing the RAC due to the higher cell count. These two factors are heavily weighted in determining the final score. Figure 4.1 plots the number of batteries in use to the predicted total score.

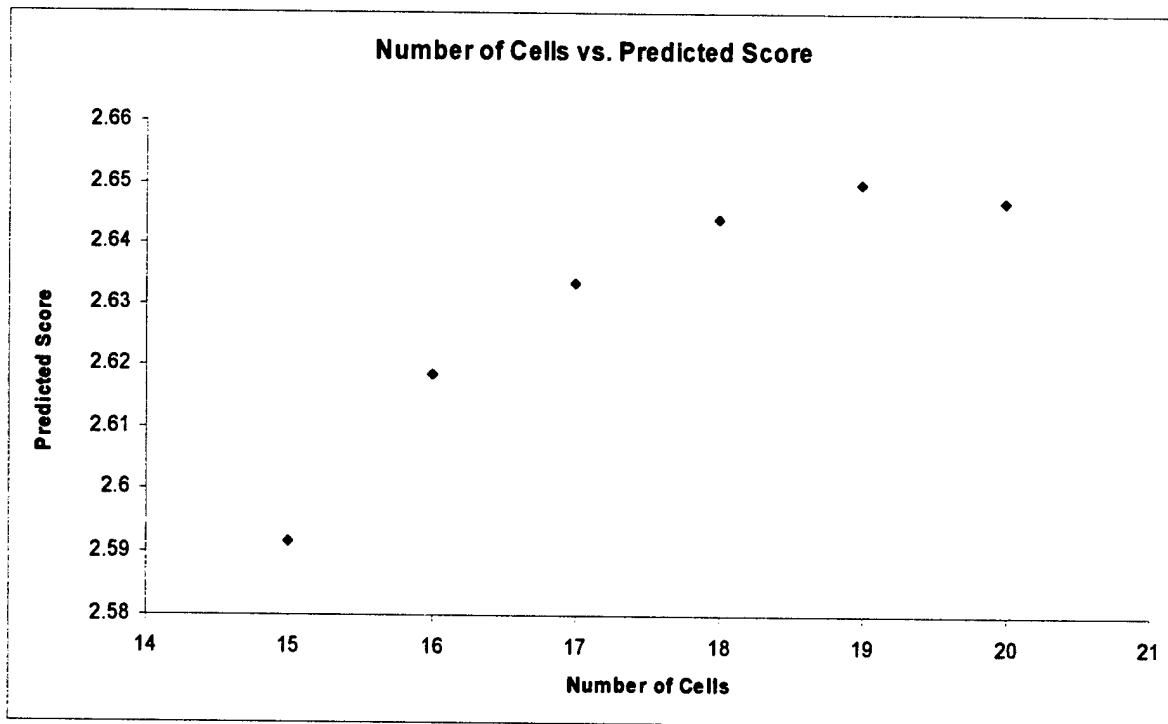


Figure 4.1: Plot of the Number of Cells vs. Predicted Score

By our predictions, the optimum number of batteries to provide the best score is 19 cells. Beyond 19 cells, the weight and number of the batteries becomes a larger factor into the RAC, reducing the overall score.

4.2 Motor Selection

Trade studies and data analysis were performed before selecting the motor that would power this years plane. Three motors were considered: Graupner 3300/5, Graupner 3300/6, and Graupner 3300/7. The motors were compared based on their maximum efficiencies, prop pitch speed, and the prop in-flight thrust. The rules state that there must be a 40 Amp (A) fuse to regulate the current draw of the motors. The three motors were analyzed in Electric Motor Calculator and were given 2:1 gear ratios based on the 40 A fuse limit. Below is a table of the properties of the motors using nineteen Sanyo 2400 mAh Ni-Cad cells (Table 4.1).

Table 4.1: Comparison of three Graupner Motors

Motors	Efficiency (%)	Prop Pitch Speed (mph)	Prop Flight Thrust (lb)
Graupner 3300/5	71.9	52.5	5.34
Graupner 3300/6	68.3	50.4	4.92
Graupner 3300/7	76.9	51.9	5.21

When the three motors were weighed against each other, the Graupner 3300/5 with a gear ratio of 2:1 produced the most desirable values for the task at hand. It is predicted to produce more in-flight thrust

and prop pitch speed than the Graupner 3300/6 and Graupner 3300/7 models while the efficiency is only 5% less than that of the Graupner 3300/7, making the Graupner 3300/5 our motor of choice.

4.3 Trade Study of Planform Area

A trade study analysis was preformed in order to get a better idea of what the dimensions of the wing should be and how it would affect the team's overall score. A range of different wingspans and chord lengths were chosen to calculate a range of planform areas in a spreadsheet; both the wing span and the chord length gave a range of planform areas of 5 to 16 square feet. A range of estimated weights of the airplane based on components parts, the size of those components, and the material makeup of those components was ranged appropriately with the planform area in order to get truer results. Using the velocity equation for the endurance properties of a propeller aircraft, a range of velocities for each planform area was calculated (Eq. 4.3).

$$V = \sqrt{\frac{2 \times W}{\rho \times S \times C_L}} \quad \text{where} \quad \begin{aligned} W &= \text{instantaneous weight} \\ \rho &= \text{density of air} \\ S &= \text{planform area} \\ C_L &= \text{maximum coefficient of lift} \end{aligned} \quad (4.3)$$

From the velocity and an approximated distance of 2300 feet, an estimated time was calculated. From this estimated time for each planform area, a single flight score was calculated for the Missile Decoy mission. It was assumed that the Difficulty Factor would level the scoring gap between the missions and the estimated Paper Score was to be 85. A plot was created for the single flight score versus planform area (Fig. 4.2).

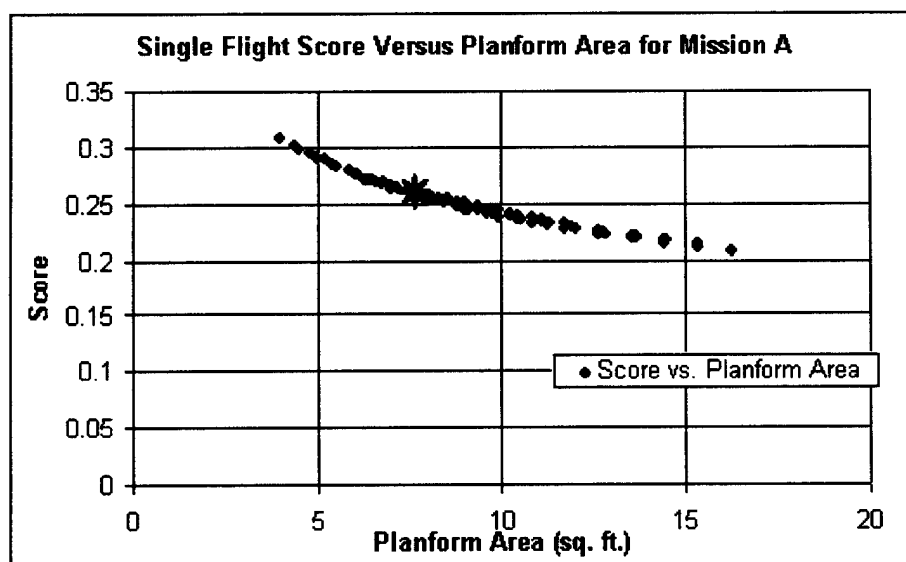


Fig. 4.2: Planform Area vs. Predicted Score

Even though the smallest planform area would raise the single flight score the most due to its decreased weight and RAC score, there is a minimum planform area that would make it unacceptable as flight would be unattainable. If the planform area is too small it will be unable to lift the airplane weight; therefore a planform area under 6 square feet can not be used. Also, with a smaller planform area there would not be enough lift for the airplane to take off in the limited runway length of 120 feet. Thus, anything less than a planform area of approximately 7 square feet could not be used. The team chose the minimum planform area that would give the proper amount of lift for the airplane to take off at 120 feet as well as correspond to the trade study of the aspect ratio (Fig. 4.3).

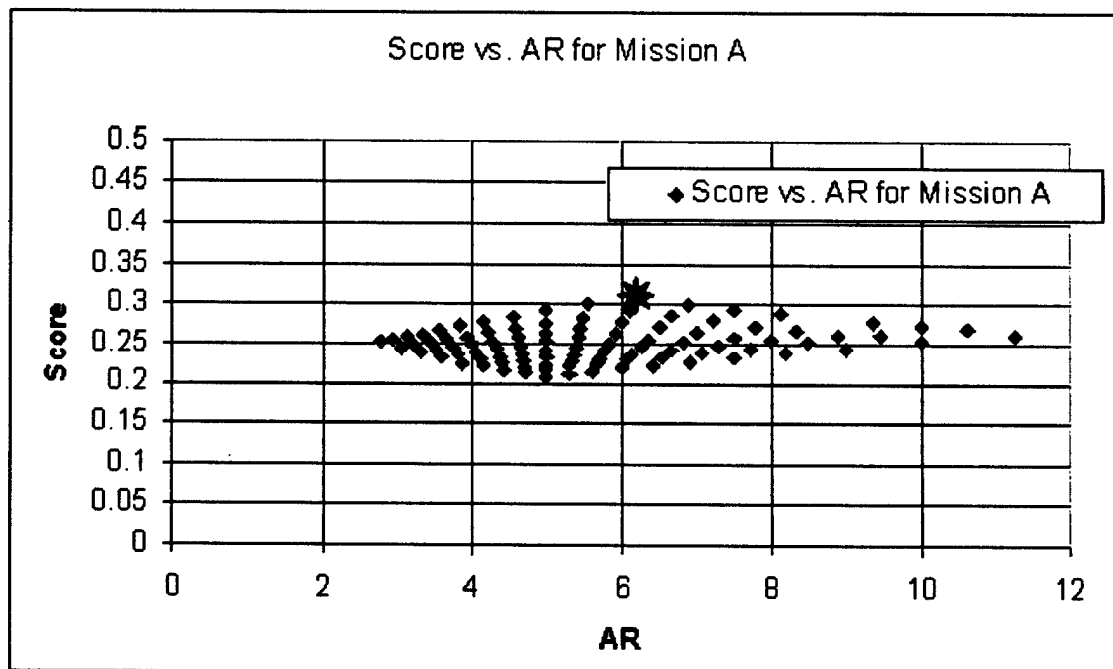


Fig. 4.3: Aspect Ratio vs. Predicted Score

The conclusion was to have the airfoil between 7.5-7.8 square feet which was in the range of a 6.2-6.3 aspect ratio.

The airfoil for this year's airplane, the S4022, showed that it has better lift properties than last year's airfoil, the Eppler 212 airfoil, which was as evident in the results of the lift to drag ratio plot (Fig. 5.4). Comparing the airplane properties of UCSD's 2002 Design/Build/Fly competition airplane, TLAR 3, the S4022 airfoil will fly equivalently, if not better. TLAR 3 had a wingspan of 8 feet and a chord length of 14 inches. From the comparison, the trade study data was reasonable and was therefore accepted. The chord was finalized at 1.1 feet or 13.2 inches, and the wingspan was finalized at 7 feet. The planform

area would then be 7.7 feet with an aspect ratio of 6.36. Further analysis on the lift and drag coefficients C_L and C_D can be found in Detailed Design 5.2.

4.4 Optimizing Tail Size

The sizing of the tail was determined by aerodynamic characteristics needed for stable flight. Initial design began with the sizing of the vertical and horizontal stabilizers. Next, the control surfaces and the placement of the tail from the center of gravity were considered. Below are Equations 4.4 and 4.5 used to calculate the planform areas of the horizontal and vertical stabilizers respectively.

$$Area_{HorizontalStabilizer} = \left(Coefficient_{HorizontalVolume} \right) \left(MAC_{MainWing} \right) \left(Area_{MainWing} \right) / \left(Arm_{HorizontalStabilizer} \right) \quad (4.4)$$

$$Area_{VerticalStabilizer} = \left(Coefficient_{VerticalVolume} \right) \left(Span_{MainWing} \right) \left(Area_{MainWing} \right) / \left(Arm_{VerticalStabilizer} \right) \quad (4.5)$$

The airfoil selected is the same for both the vertical and horizontal stabilizers. The Selig S9027-8 was chosen because it is symmetric and therefore its aerodynamic properties could be modified during flight by the aileron or rudder. The volume coefficients were mirrored after historical values for home built aircraft which were 0.50 and 0.04 for the horizontal and vertical stabilizers respectively. The tail arm is 31.5 inches which yielded an area of 232.3 in² and 88.7 in² for the horizontal and vertical stabilizers, respectively.

The horizontal stabilizer is not tapered and has an aspect ratio of 1.9. The span and tail chord are 21.0 and 11.1 inches, respectively. The vertical stabilizer is slightly tapered to strengthen the tail geometry. For low-speed aircraft very little taper is needed, if at all. The taper ratio for the tail is 0.80 with a sweep angle of 15.0 degrees. The vertical stabilizer's aspect ratio is 1.1 which is high via historical data for T-tails. The span of the vertical tail is 10.0 in. The calculated root and tip chord for the tapered vertical stabilizer is 11.1 and 8.9 in, respectively.

4.5 Payload Deployment System

The proposed payload deployment system requires a servo to pull a pin from a hole in the tab, causing the payload to drop directly down. Figure 4.10 depicts the side, top, and front view of the payload deployment system. When activated the servo pulls a pin from the tab releasing the payload. Two servo models and two solenoid models were tested to determine if they were able to reliably pull a pin from the tab of the payload. The servo or solenoid must overcome approximately 1 lbf of friction to be able to pull

the pin from the tab. A Hitec HS-55 servo with a torque of 15 / 18 oz-in. was first used, but it was not strong enough to perform the task. A Hitec HS 81MG servo with a torque of 36 / 42 oz.-in. was able to perform the task. Both of the solenoid models, however, were not able to pull the pin from the tab, and the masses of both of the solenoids were too large to even be considered in the deployment system design. Below is a table of the results of the testing (Table 4.4).

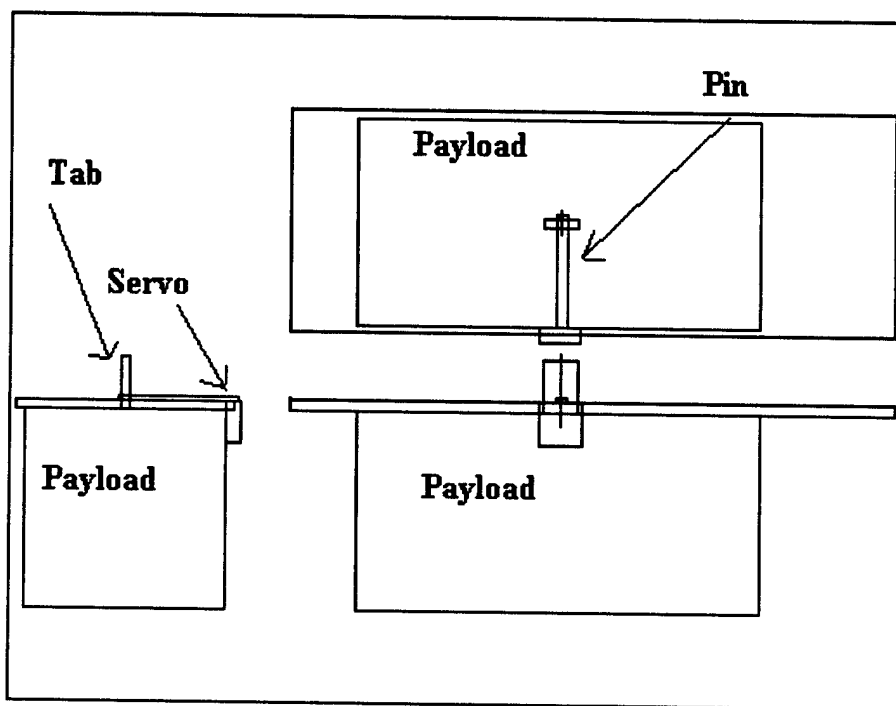


Figure 4.4: The payload deployment system.

Table 4.4: Deployment Mechanisms Considered and Tested

Model	Description	Result
Hitec HS-81MG	Torque = 36 / 42 oz.-in.	Successfully deployed.
Hitec HS-55	Torque = 15 / 18 oz.-in.	Torque was too low.
24 DC Solenoid	Force = 40 oz.	Payload jammed.
12 DC Solenoid	Force = 80 oz.	Too bulky to test.

After the risk reduction testing was performed, it was determined that Hitec HS-81MG or a servo with higher torque should be used to release the payload from the tab.

4.6 Spar Analysis and Optimization

The spar was analyzed based on the properties of balsa wood, which is the material to be used to construct the spar and wing joiner. Because the balsa wood will carry the load of the aircraft, the spar and wing joiner must be able to withstand the predicted maximum bending moment under the weight of the aircraft estimated at approximately 17 lb (75.7 N) with the payload and undergoing 3 g of acceleration. It can be assumed that the two spars are beams under constant upward load, bending moment, and torsion. The two spars are joined by a wing joiner. The point where the spar is most likely to fail under constant bending moment is at the center of the two joined spars. Equation 4.7 describes the maximum moment at the center of the spar located in the fuselage where F is the load and L is the total length of the two spars combined.

$$\text{Maximum Moment: } M = \frac{3}{4} * F * L \quad (4.7)$$

Below are the relevant estimated dimensions for the aircraft to determine the bending moment M (Table 4.5).

Table 4.5: Relevant Dimensions to Estimate the Bending Moment

Description of Components	English Units	Metric Units
Total Length of Spars	84 in.	2.14 m
Estimated Weight with Payload	17 lbs	76 N
w (N/m)	0.202 lb/in	35.5 N/m
Bending Moment M	1,070 lb-in	122 N-m

To determine the optimal cross-section for the spar structure, stress and static analyses were conducted. Optimization of the spar cross section involved determining the maximum stresses during banked turns, which is estimated at 3 g of acceleration. Equations 4.8 and 4.9 were utilized to determine the values of stress and moment of inertia under the maximum bending moment respectively.

$$\text{Maximum Bending Stress: } \sigma = \frac{Mc}{I} \quad (4.8)$$

$$\text{Moments of Inertia of a Rectangular Cross Section: } I = \frac{1}{12}bh^3 \quad (4.9)$$

In optimizing the cross-section, a factor of safety of 1.5 was used to be able to withstand bending moments and torsions. The ultimate tensile strength of carbon fiber in 0, 45, and 90 degree orientations is approximately $\sigma_y = 2900$ MPa, and the ultimate tensile strength of medium density balsa is 19.2 MPa. The maximum tension and compression is located a length c from the axis (Fig. 4.5).

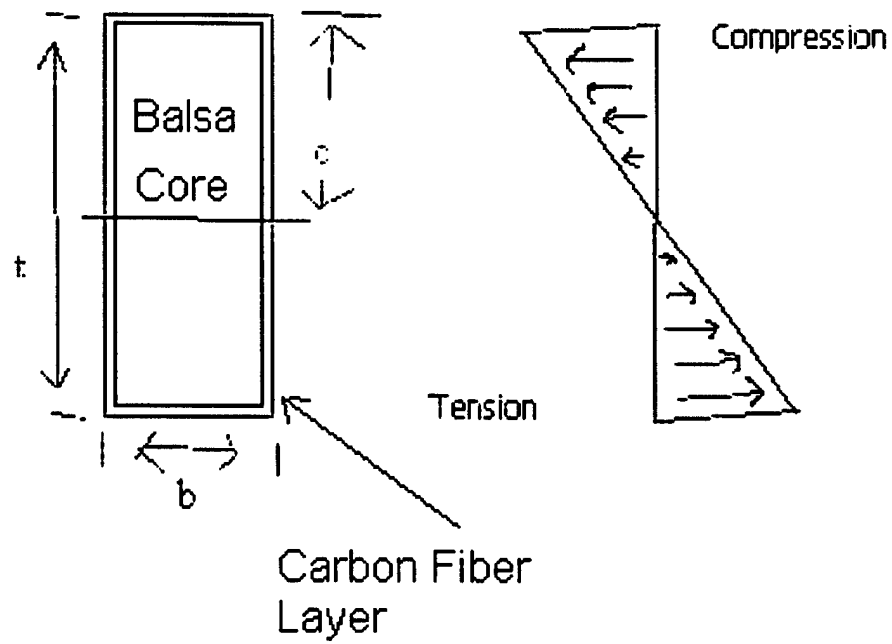


Figure 4.6: Cross section of the spar

The vertical length t of the cross section is 1.7" (43.2 mm). From the properties of balsa, a length b can be determined (Eq. 4.10).

$$b = \frac{12 * M * c * FS}{\sigma_y * t^3} \quad (4.10)$$

where $FS = 1.5$, $c = \frac{t}{2}$, and σ_y is the yield strength of balsa

Based on Equation 4.8, the base length b of the cross section was found to be 1.34" (34.2 mm). Because the weights and bending moments are only estimates, it is probably more advisable to further strengthen the spar by glassing with a thin layer of uni-directional carbon fiber around the balsa core. Therefore, the final dimension of the cross section of the spar is 1.8" x 1.3" (45.7 mm x 33.0 mm) with the added layers of carbon fiber. The structural integrity of the spar and wing joiner is vital to the overall aircraft because the majority of the loads during flight is concentrated in the spar and wing joiner. Optimizing the spar and wing joiner can insure that the structure does not fail.

5.0 Detailed Design

Under the Detailed Design Phase, the vital statistics of the aircraft are given. The Aerodynamics sub-team evaluated the pitching moment coefficient C_M , coefficient of lift C_L and the coefficient of drag C_D under various angles of attack and velocities. The Propulsion sub-team selected the motor, propeller, and batteries to be used. The Controls/Stability sub-team analyzed the center of gravity of the aircraft when empty, with the payload, and fully loaded with the payload and antenna based on the weight estimates. The Structures sub-team provided a detailed geometric sizing of the aircraft, its payload deployment system, and the Rated Aircraft Cost (RAC).

5.1 Summary of Aircraft Geometry and Features

The Furious Flier aircraft was designed to fulfill the requirements and constraints of the 2003 Design/Build/Fly rules. It was designed to fit within a 4'x2'x1' storage container, to assemble with the quickest time possible while out of the container and to perform the Missile Decoy and Sensor Deployment Missions. Some distinct features of this aircraft include an externally mounted payload, high mounted wing, rear landing gears to allow clearance for the 6"x6"x12" payload when it is deployed, a detachable T-tail boom with a horizontal tail span of 21", vertical tail span of 10", a Graupner 3300/5, two propeller blades with a total span of 18" and 13" pitch. The payload is released by activating a high-torque servo which pulls a pin from a hole in the tab, causing the payload to drop directly down and a door-like structure to close the opening of the aircraft. The simulated antenna is made from a 6" Schedule 40 PVC pipe that is 3" high with 1/16" thick birch plywood closing the simulated antenna as specified in the rules. Two polyurethane columns reinforced by uni-directional carbon fiber composites hold up the simulated antenna in place. Detailed descriptions of the dimensions of the fuselage, wings, tail, and weight estimates can be found further in the Detailed Design 5.1.1—5.1.4. Below are Tables 5.1 through 5.4 summarizing the basic dimensions of the fuselage, wings, tail, and weight estimates while a Three-View Drawing of the aircraft can be found in Drawing Package 5.7.1.

Table 5.1: Fuselage Sizing

Description	English	Metric
Length from nose to tail	53 in (4.42 ft)	1.346 m
Width	6.5 in (0.542 ft)	0.165 m
Total Height	12.5 in (1.04 ft)	0.318 m

Table 5.2: Wing Sizing with a S4022 Airfoil

Description	English	Metric
Chord Length	13.3 in (1.1 ft)	0.335 m
Total Span	84 in (7 ft)	2.134 m
Area	1108.8 in ² (7.7 ft ²)	0.715 m ²
Aspect Ratio	6.36	6.36
Taper Ratio	1	1
Control Area per Wing	84 in ² (0.583 ft ²)	0.054 m ²

Table 5.3: Empenage Sizing with a S9027 Airfoil

Description	English	Metric
Tail Arm	31.5 in (2.63 ft)	0.8 m
Horizontal Taper Ratio	1	1
Horizontal Area	232.3 in ² (1.613 ft ²)	0.150 m ²
Horizontal Aspect Ratio	1.9	1.9
Horizontal Tail Span	21.0 in (1.75 ft)	0.533 m
Horizontal Tail Chord	11.0 in (9.21 ft)	0.281 m
Vertical Area	88.7 in ² (0.616 ft ²)	0.0572 m ²
Vertical Aspect Ratio	1.127	1.127
Vertical Taper Ratio	0.8	0.8
Vertical Tail Span	10 in (0.833 ft)	0.254 m
Vertical Chord Tip	8.87 in (0.739 ft)	0.225 m
Vertical Chord Root	11.09 in (0.924 ft)	0.282 m
Vertical Tail Sweep	15°	15°

5.1.1 Fuselage Features

The fuselage consists of two compartments with specific functions. The top compartment, which is approximately 1.8" high, 6.5" wide, and 16" long is the "backbone" structure of the aircraft, containing the wing joiner and holding the tail's boom in place. Because the lower plate of the upper compartment has to undergo moment, torsion, and shock loads from the wings, tail boom, rear landing gears and motor, the plate of the lower floor is composed of dense polyurethane material reinforced by uni-directional carbon fiber at 0° and 90° orientations and bi-directional carbon fiber at 45° and 135° orientations. According to Matweb.com, polyurethane with carbon fiber reinforcement has an ultimate tensile strength of between 55—248 MPa. Because of the high density of polyurethane with carbon fiber reinforcement, which is between 0.0444—0.0495 lb/in³ (1.23—1.37 g/cc), only one plate was used to provide structural support. Making all of the walls of the upper compartment out of this material would

add unnecessary weight to the aircraft. The side and upper plates of the upper compartment is composed of dense foam sandwiched by uni-directional and bi-directional carbon fiber which would provide support under shear stress. The purpose of the bottom compartment, which is 1.25" high, 6.5" wide, and 16" long, is to hold the nineteen nickel-cadmium cells, receivers, speed controllers, and payload tab in place. The payload is actually located below the bottom compartment while the tab of the payload protrudes into the bottom compartment secured by a pin fastened onto a high torque servo. Once activated, the servo pulls the pin from the hole in the tab allowing the payload to drop. Enough gap space between the cells to prevent the battery cells from interfering with the motion of the pin. The manufacturing process of the spar/wing joiner, fuselage, boom, and landing gears can be found in Manufacturing FF's Wings and Empennage 6.2.2, 6.2.3, 6.2.4, and 6.2.5 respectively while a detailed 3D model of the wings can be found in the Drawing Package 5.7.4.

5.1.2 Wing Features

The wings were designed to be quickly mounted onto the wing joiner of the fuselage once taken out of the 4'x2'x1' shipping container. The spars which are made from balsa reinforced by uni-directional carbon are secured by two pins inside of the wing joiners. The wing ribs and torsion pin provide stiffness under torsional loads while the cross section of the spar is optimized to perform under moment. The wings are cut from low density white foam and glassed with fiber glass and epoxy. The manufacturing process of the wings and empennage can be found in Manufacturing FF's Wings and Empennage 6.2.1 while a detailed 3D model of the wings can be found in the Drawing Package 5.7.4.

5.1.3 Tail Features

The main feature of the tail is that it is detachable from the fuselage and is held in place by bulkheads while in the fuselage. The carbon fiber boom provides stiffness while undergoing bending and torsion. The vertical and horizontal stabilizers are cut from low density foam and glassed with fiber glass to give it structural support. The manufacturing process of the wings and empennage can be found in Manufacturing FF's Wings and Empennage 6.2.1 while a detailed 3D model of the wings can be found in the Drawing Package 5.7.5.

5.2 Assessing the Airfoil Properties

Assumptions were made based on medium properties and on theoretical software of VisualFoil version 4.0. VisualFoil is simulation software that can analyze and compare airfoils. The majority of the preliminary aerodynamic features of the aircraft came from the results of VisualFoil.

The environmental properties and flight conditions were the first assumptions determined. Air properties were taken at sea level. From the experience of flying previous design/build/fly airplanes and from the power of the batteries and motor, a predicted cruise velocity of the designed airplane was

estimated to be 50 miles per hour. The Reynold's number was calculated from the estimated flight conditions and the estimated cruise velocity (Eq. 5.1).

$$Re = \frac{\rho_\infty \times V_\infty \times c}{\mu_\infty} \quad \text{where } \begin{aligned} \rho_\infty &= \text{freestream density} \\ V_\infty &= \text{Velocity at the freestream velocity} \\ c &= \text{chord length} \\ \mu_\infty &= \text{freestream viscosity} \end{aligned} \quad (5.1)$$

The Reynold's number calculation determined the airfoil the final airfoil. With VisualFoil, different airfoil properties were observed by the members of the aerodynamic group. The S4022 showed a low drag coefficient, a high maximum lift, and good stall characteristics for the predicted Reynold's number. Therefore, the aerodynamic group agreed the S4022 would give the best aerodynamic qualities in the airplane design.

The VisualFoil software produced data for the coefficient of lift, the coefficient of drag, and the coefficient of the pitching moment at the quarter chord at various speeds. To see changes in the coefficient properties from 50 miles per hour, 30 miles per hour and 40 miles per hour were the chosen speeds to take coefficients. Through Microsoft Excel 2002, data tables and plots were created for the coefficient of lift, the lift to drag ratio, and the center of pressure against each angle of attack (Fig. 5.1). In figure 5.1, maximum coefficient of lift was determined by the average of the point before the plots change directions. The angle of attack where the maximum coefficient of lift occurs shows the maximum angle of attack the airfoil can go to maintain the greatest lift. When the curve peaks stalling occurs. The maximum coefficient of lift for 30mph, 40mph and 50mph averages to 1.6 (5.1).

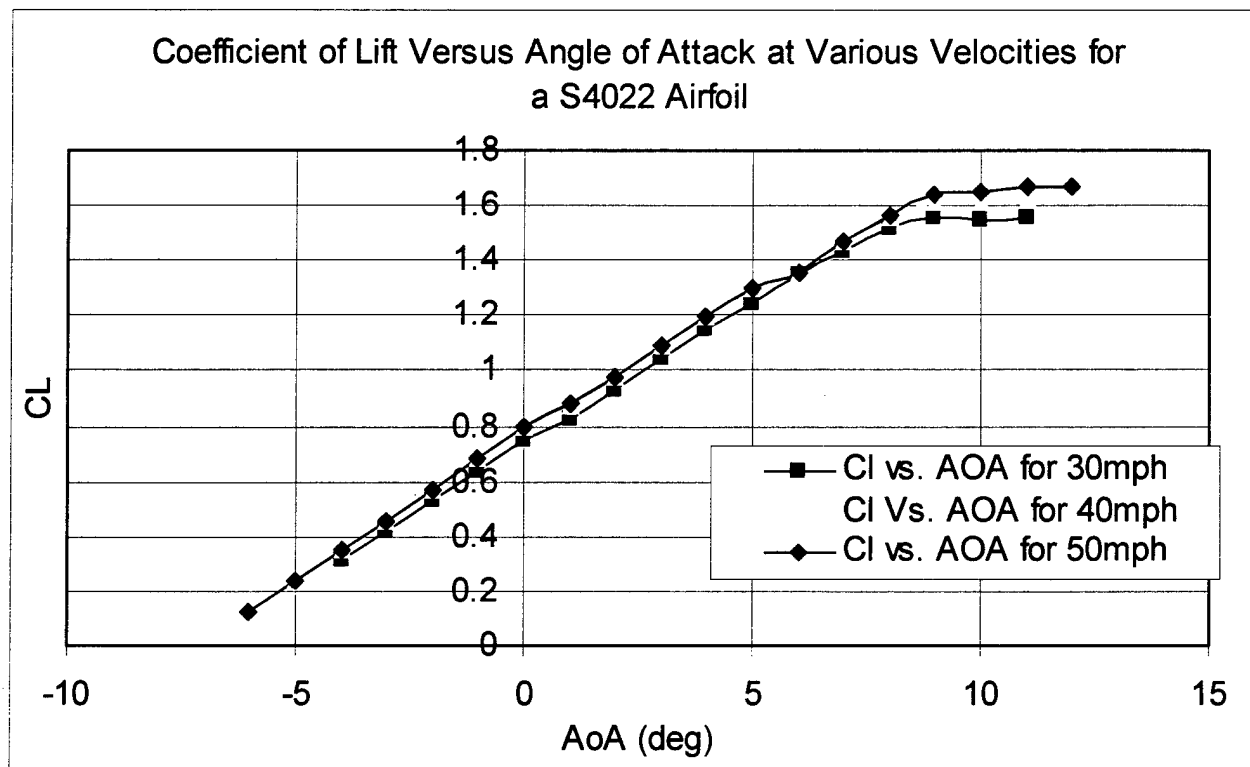


Figure 5.1: Coefficient of Lift C_L vs. Angle of Attack AOA

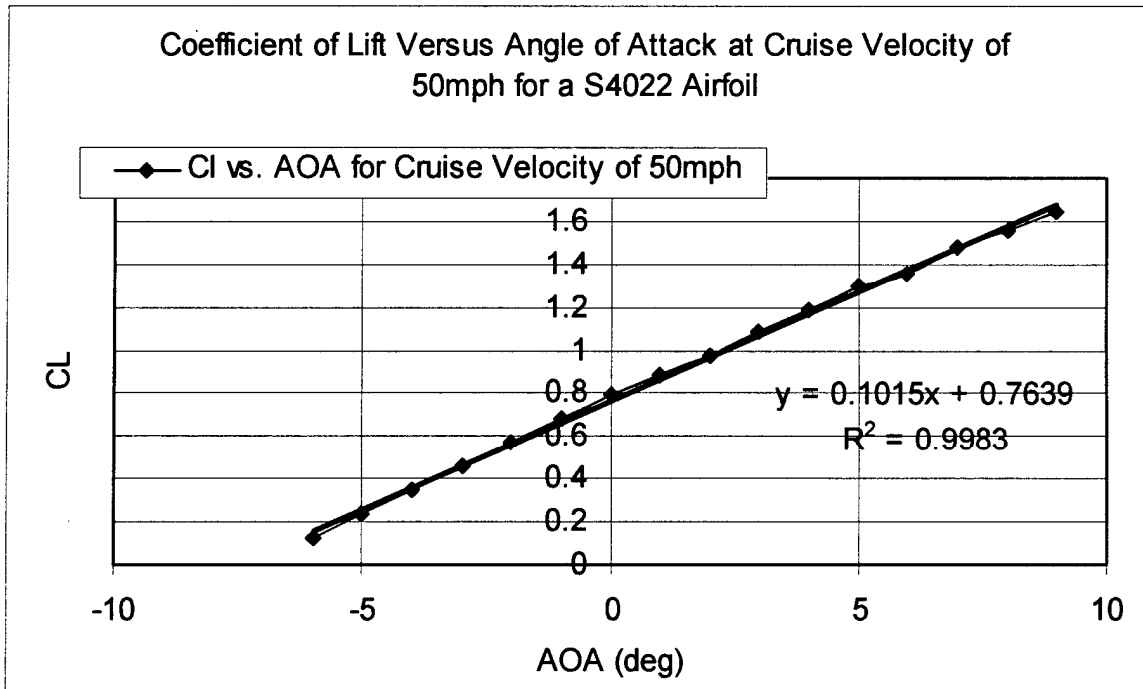


Figure 5.2: Coefficient of Lift C_L at Cruise Speed vs. Angle of Attack AOA

The coefficient of lift versus angle of attack at cruise velocity of 50 miles per hour is singled out to show the best fit line. The best fit line and equation is used in calculations of finite wing.

The pitching moment can essentially be anywhere on the chord line at different angles. The pitching moment taken from the VisualFoil was calculated at the quarter chord. The pitching moment coefficient has a gradual increase at each angle of attack for each of the velocities. The pitching moment is small compared to other airfoils as can be seen in the plot of $C_m, c/4$ versus angle of attack (Fig. 5.3).

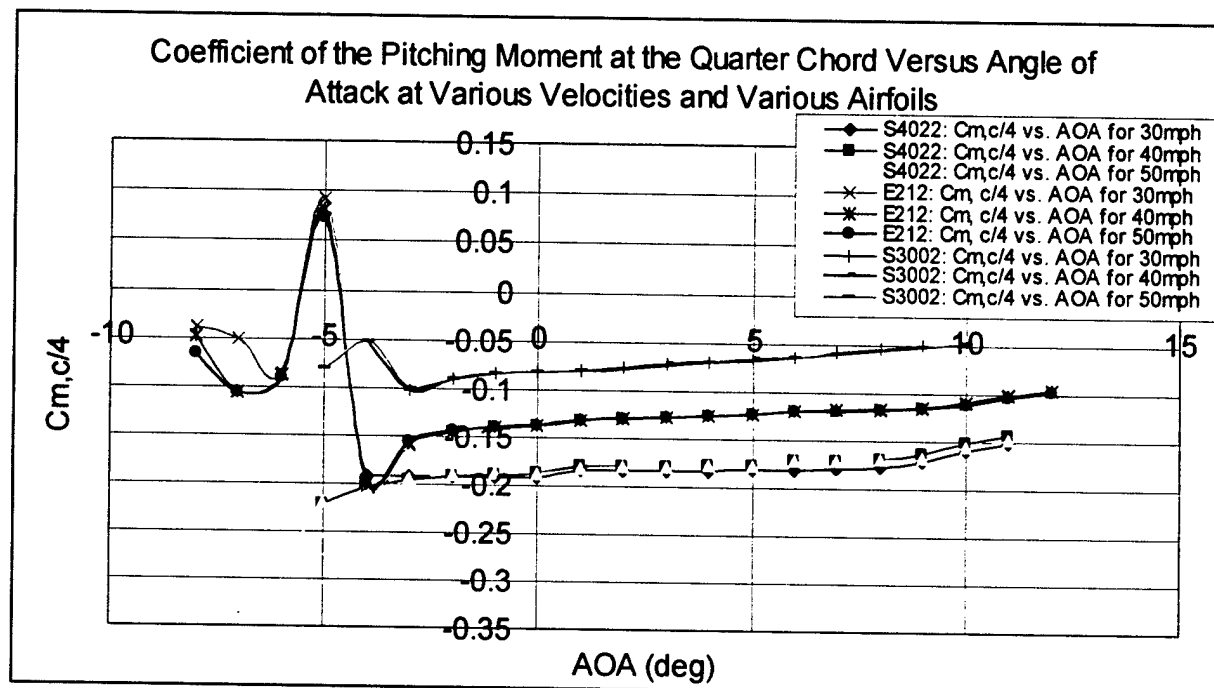


Figure 5.3: Coefficient of Pitching Moment at the Quarter Chord $C_m, c/4$ vs. Angle of Attack AOA

To plot the lift to drag ratio, an aerodynamic group member used the coefficient of lift and the coefficient of drag from the VisualFoil data. Below is a plot of the lift to drag ratio of the chosen airfoil S4022 (Fig. 5.4).

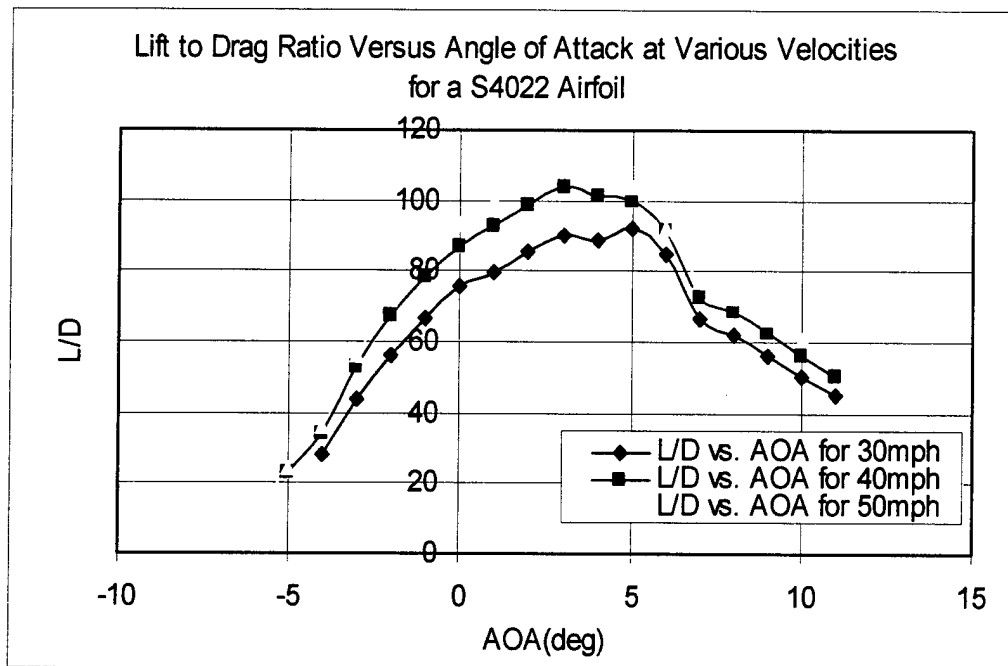


Figure 5.4: Lift to Drag Ratio vs. Angle of Attack AOA

From the lift to drag ratio versus angle of attack plot, a new plot of maximum lift to drag ratio versus velocity was created (Fig. 5.5).

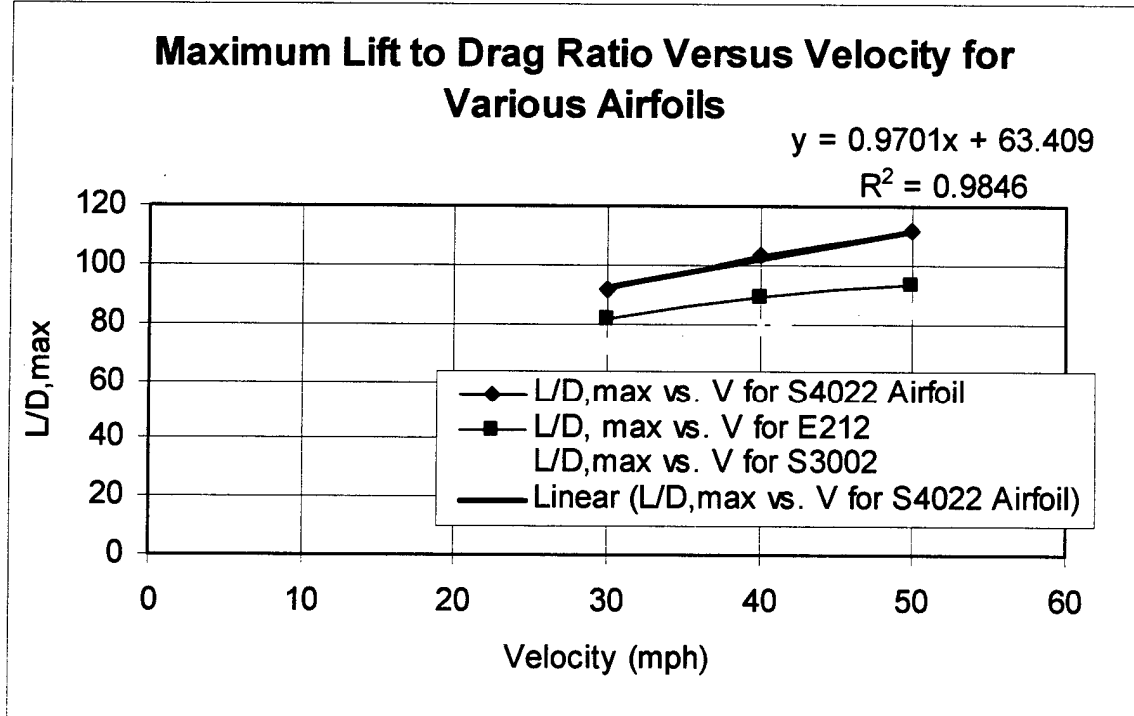


Figure 5.5: Lift to Drag Ratio for Various Airfoils

Other maximum lift to drag ratios for different velocities was done for the E212 airfoil and the S3002 airfoil to compare the better aerodynamic properties of the S4022 airfoil that was chosen. The lift to drag ratio is a true measure of the aerodynamic efficiency of a body shape. The higher $(L/D)_{max}$ for any given velocity, the more aerodynamically efficient is the body. This analysis of the lift to drag ratio only corresponds to the S4022 airfoil alone. The actual body of the airplane will cause the maximum lift to drag ratio to reduce for each speed.

The center of pressure was calculated for each angle of attack using the Equation 5.7.

$$X_{cp} = chord \times \left(\frac{1}{4} - \frac{C_{m,c/4}}{C_L} \right) \quad (5.7)$$

Below is a plot of the Center of Pressure vs. Angle of Attack AOA (Fig. 5.6).

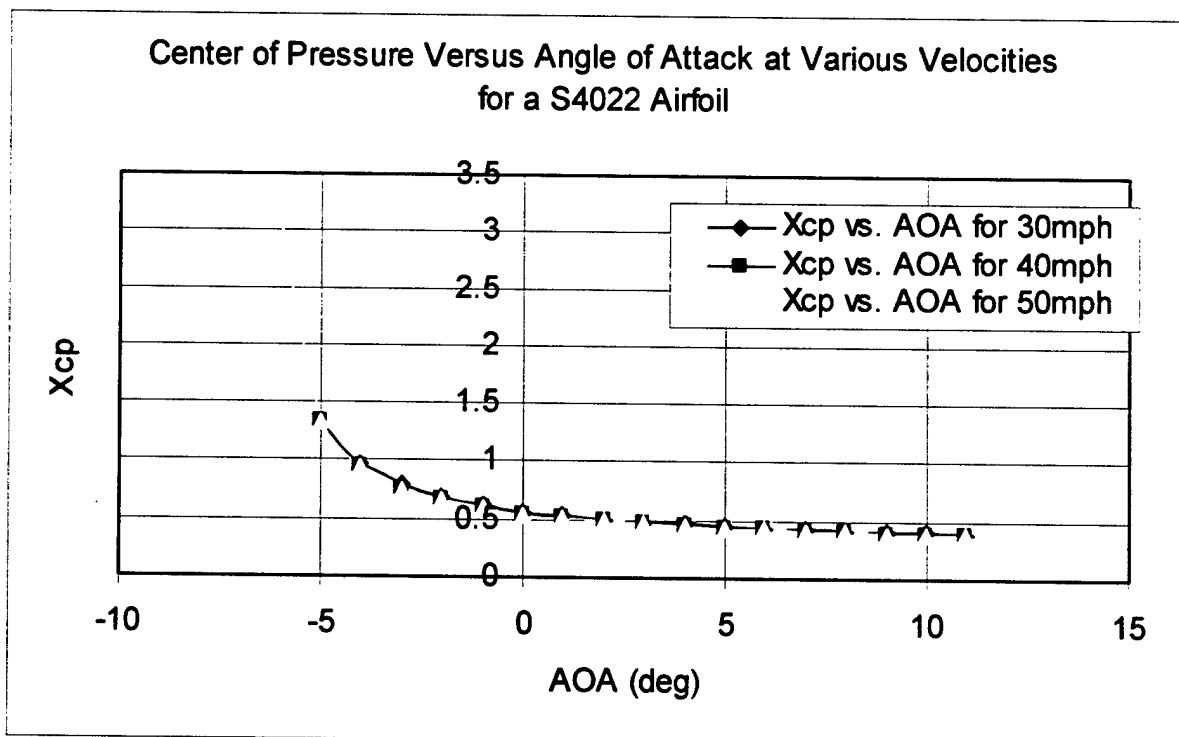


Figure 5.6: Center Pressure vs. Angle of Attack

The center of pressure is the location where the resultant of a distributed load effectively acts on the body. It is also a point on the body about which the aerodynamic moment is zero. The center of pressure changes with the angle of attack. In general, from the plot, the center of pressure moves closer to the leading edge as the angle of attack increase. The center of pressure seems to stabilize a certain distance from the leading edge before stalling, and the center of pressure never goes beyond the leading edge or trailing edge. From this interpretation and analysis, the airfoil is very stable in flight.

5.3 Properties of the Propulsion System

The configuration of the propulsion system was based on the power management, efficiency, and RAC concerns. The maximum propeller span of 18" was selected while the 13" pitch was selected based on achieving a 50 mph flight. The total power available to the Graupner 3300/5 is given by $P = I \cdot V = 731$ Watts while the power out is approximately 540 W. The final thrust-to-weight ratio is 0.27. Nineteen Sanyo 2400 mAh batteries will be used to supply the power because of their high energy density of 1.11 Wh/oz. The maximum efficiency is achieved when the motor is at 12000 RPM.

5.4 Static Stability

The static stability of the aircraft, i.e. the ability of the aircraft to remain in stable flight after wind disturbances, is an important aspect of the design. The first step was to calculate the Center of Gravity (CG). To do so the masses and location of every part of the plane were measured and recorded in Table 5.4.

Table 5.4: Weight Estimation of Aircraft Parts

Weight Estimation			
Part	Station	Weight	Moment
Propulsion			
Propeller	0 In	8 oz	0 in-oz
Motor	2.5 In	21 oz	52.5 in-oz
Batteries	11 In	45 oz	495 in-oz
wiring harness	16 In	2 oz	32 in-oz
Fuselage			
fuselage shell	12 In	10 oz	120 in-oz
Backbone	12 In	20 oz	240 in-oz
landing gear	10 In	16 oz	160 in-oz
nose gear	5 In	5 oz	25 in-oz
Avionics			
speed controller	7 In	6 oz	42 in-oz
Receiver	7 In	1.65 oz	11.55 in-oz
wing servo	13 In	2 oz	26 in-oz
tail servo	47 In	1 oz	47 in-oz
payload servo	12 In	2 oz	24 in-oz
Payload			
Payload	12 In	80 oz	960 in-oz
antenna mount	12 In	2 oz	24 in-oz
Antenna	12 In	16 oz	192 in-oz
trap door	13.5 In	6 oz	81 in-oz
Aircraft Structures			
Wing	12 In	30 oz	360 in-oz
Boom	28.85 In	5 oz	144.25 in-oz
Empennage	47 In	10 oz	470 in-oz
Total Weight		287.65 oz	
		17.98 lbs	

The moment is calculated about the front tip of the aircraft. The sum of the moments about CG is zero. CG is calculated through Equation 5.8.

$$CG = \frac{\sum_{i=1}^n (Moment)_i}{\sum_{i=1}^n (mass)_i} \quad (5.8)$$

Three different CG's were calculated—empty, with payload, and with payload and antenna—and are listed in Table 5.3.

Table 5.5 Center of Gravity

CG			
	Weight (oz)	weight (lbs)	CG (in)
empty	192.65	12.040625	12.22061
w/payload	272.65	17.040625	12.15588
w/payload & antenna	288.65	18.040625	12.14724

With CG calculated, the stability of the aircraft was analyzed. Stability was analyzed in 3 directions: rolling, pitching, and yawing.

The aircraft is completely symmetric about the x-z plane (x direction positive is from CG to the front of the aircraft, y direction positive is from CG out through the right wing, and z direction positive is from CG pointing downward normal to level flight), therefore roll stability is achieved without any aileron deflection provided there are no perturbations in wind or pressure. Since that is only a theoretical condition, the ailerons are deflected to offset the rolling moment created by changes in wind or pressure. The ailerons are placed near the ends of the wings so that little deflection is needed to get a large rolling moment on the aircraft.

The pitching stability is controlled through use of the horizontal tail and the elevators. Every lifting surface creates a moment about CG; the horizontal tail's function is to offset the moment created by the wing. The high lifting force on the wing is offset by the long moment arm set by the length of the tail boom: 37 in. This distance allows the range of the deflection of the elevators to remain small because not much lift is needed through the horizontal stabilizer. The horizontal tail surface is a symmetrical airfoil elevators are used to create camber, thus producing lift to offset the moment of the wing's lift. The elevators are also used in controlling flight against small wind disturbances and pressure fluctuations that create a pitching moment on the aircraft.

Yawing stability is maintained with the vertical stabilizer and tail rudder. The rudder and vertical stabilizer are used to avoid side slip. The rudder maintains the front of the aircraft pointing in the same

direction as the direction of flight. If there is a cross wind during flight the rudder helps to maintain a straight flight path. The deflections of the rudder, needed to produce desirable results, are small because of the long moment arm created by the tail boom. In steady level flight with no perturbations in wind or pressure, the yawing moment will be zero and there would be no use of the rudder. Unfortunately, for the ease of control and stability, this is not the case. Small deflections of the rudder are used to maintain yawing stability throughout flight.

5.5 Mission Performance

In order to evaluate and estimate our plane's performance; analysis of rate of climb, stall speed, and take-off and landing specifications was necessary. The performance calculations requires the relevant dynamic pressure taken at air properties at sea level and at the takeoff velocity. Below is the dynamic pressure (Eq. 5.9).

$$q_{\infty} = (1/2) * \rho_{\infty} * (V_{\text{takeoff}})^2 \quad (5.9)$$

The take-off and landing velocity calculations were based on the stall speed (Eq. 5.10—5.11).

$$V_{\text{takeoff}} = 1.2 * V_{\text{stall}} \quad (5.12)$$

$$V_{\text{landing}} = 1.3 * V_{\text{stall}} \quad (5.13)$$

where the level flight stalling velocity is found in Equation 5.14.

$$V_{\text{stall}} = \sqrt{(2 * \text{Weight}) / (\rho_{\infty} * S * C_{L,\max})} \quad (5.14)$$

where S = planform area

From these takeoff /landing velocities and dynamic pressures, take-off and landing distances can be found. Takeoff distance is the sum of the ground run and airborne distance. The takeoff distance should be as minimal as possible for quick and efficient operation of the aircraft.

Table 5.4 shows the performance summary of the aircraft at various stages of the mission.

Table 5.6: Predicted Performance of the Aircraft

Performance Summary			
	Empty	With Payload	With Payload and Antenna
Stall Speed	22.0 ft/s	26.2 ft/s	27.0 ft/s
Take Off Speed	32.4 ft/s	32.4 ft/s	32.4 ft/s
Take Off Lift	5.34 lbf	5.34 lbf	5.34 lbf
Take Off Drag	0.27 lbf	0.27 lbf	0.27 lbf
Take Off Distance	4.18 ft	5.93 ft	6.29 ft
Take Off Time	0.26 s	0.36 s.	0.39 s
Landing Speed	28.7 ft/s	34.1 ft/s	35.1 ft/s
Landing Distance	3.27 ft	6.58 ft	7.39 ft

It should be noted that the estimated take off distance empty, with the payload, and with the payload and antenna is approximately 4.2 ft, 4.9 ft, and 6.3 ft respectively, which should allow the aircraft to clear the 120 ft range specified by the rules.

The rate of climb (V_y) is the vertical component of the plane's true airspeed. Below is Figure 5.5, showing the components of the angle of climb.

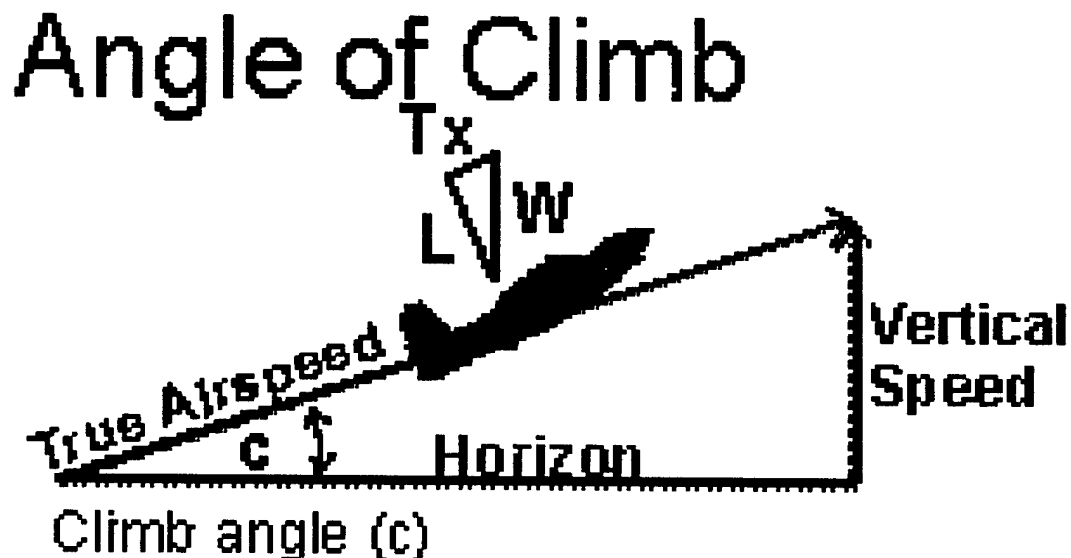


Figure 5.7: Rate of Climb Diagram

The climb angle (α) is the measured angle from the horizon to the flight path. The rate of climb can be expressed by Equation 5.15.

$$V_Y = \frac{(Thrust - Drag) * True_Air_Speed}{Weight} \quad (5.15)$$

Utilizing Equation 5.15, the rate of climb was calculated for the empty weight plane, the plane with the payload, and the plane with the payload and antenna. The rate of climb performance can be seen in Table 5.5.

Table 5.7: Estimated Rate of Climb Performance

Rate of Climb Performance			
	Empty	With Payload	Fully Loaded
Rate of Climb	13.7 ft/s	9.7 ft/s	9.2 ft/s
Climbing Distance	144 ft	209 ft	222 ft
Climb Angle	19.2 deg	13.4 deg	12.7 deg
Climb Time	1.96 s	2.85s	3.03s
Turning Radius	81.4 ft	132.0 ft	145 ft

The performance of the aircraft is critical in how well the aircraft competes in the Design/Build/Fly Competition. For example, the turning radius when empty, with the payload, and fully loaded with the payload and antenna are 81.4 ft, 132 ft, and 145 ft respectively. The smaller the turning radius, the faster the aircraft can perform its mission. The numbers are only estimates, so the properties of the performance of the aircraft can further be verified through flight testing.

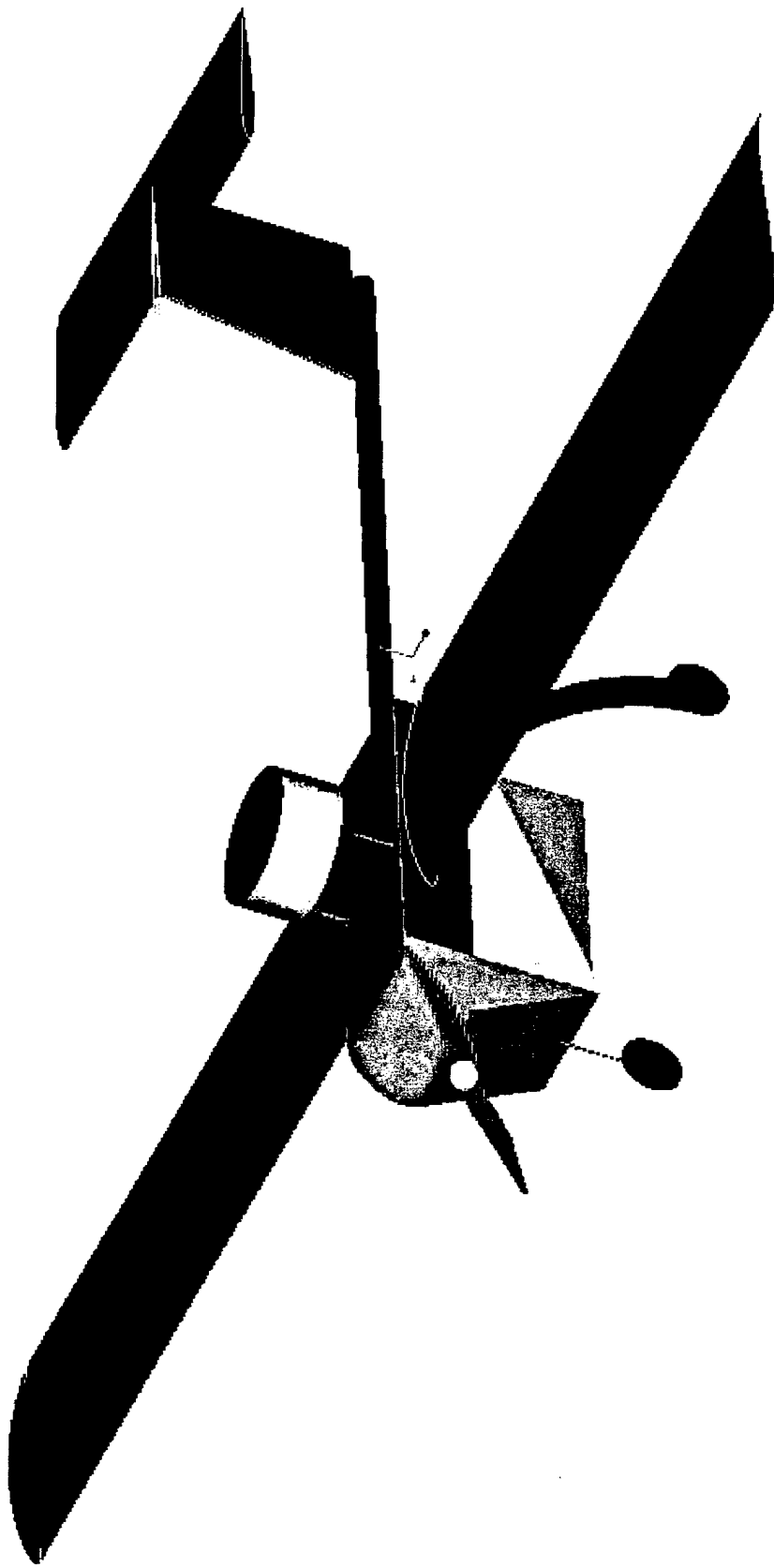
5.6 Rated Aircraft Cost

After the aircraft was designed, a more accurate value of the Rated Aircraft Cost of the design was given to be 9.774. Keeping the Rated Aircraft Cost low is essential to be competitive.

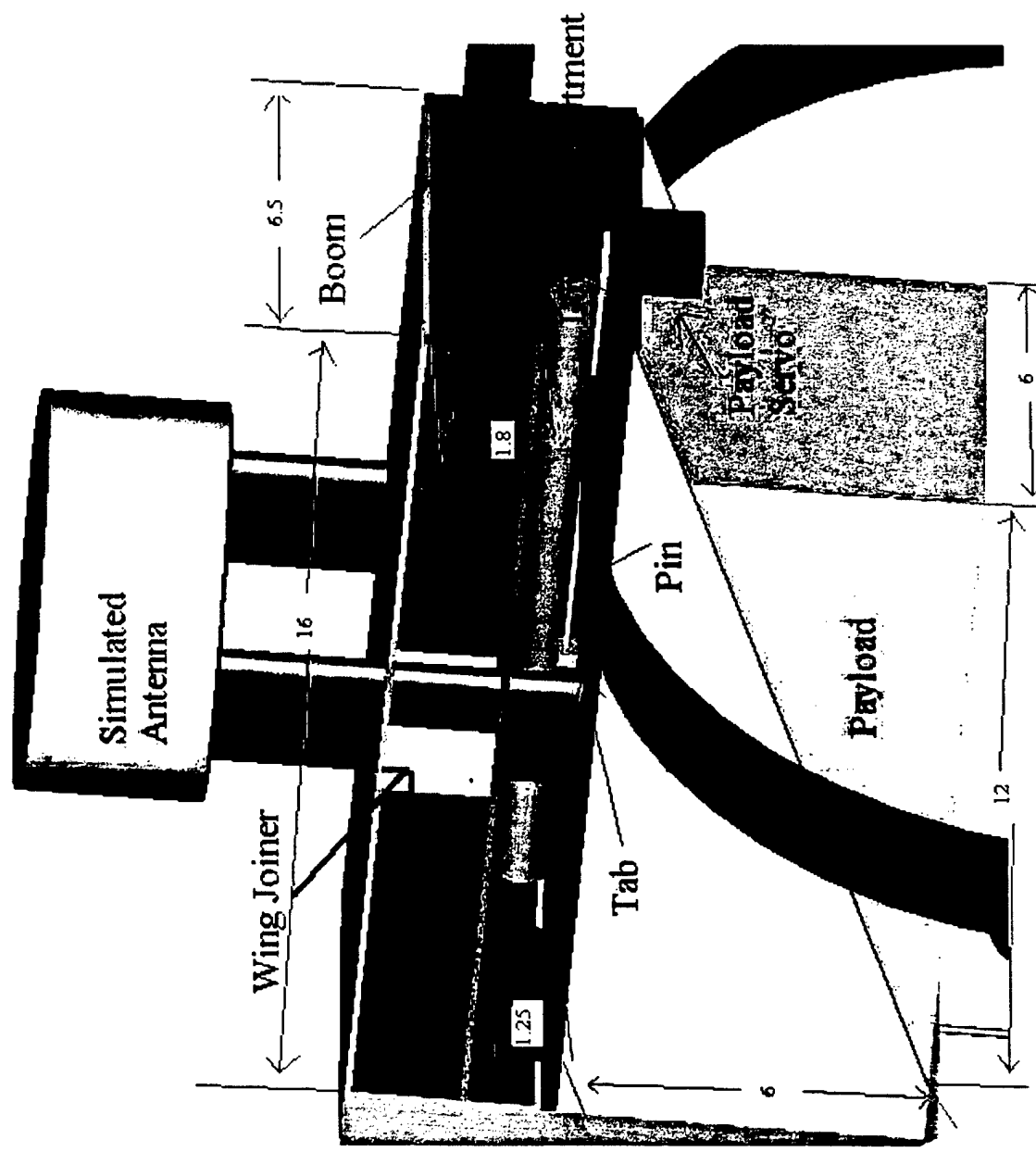
Table 5.8: Rated Aircraft Cost

Rated Aircraft Cost (RAC) = (A * MEW + B * REP + C * MFHR) / 1000 =		
9.655		
Manufacturers Empty Weight Multiplier (MEW)	A = \$ 100	
Total Weight w/o Payload =	15 lbs	
		MEW = 15
Rated Engine Power Multiplier (REP)	B = \$ 1500	
# of engines =	1	
Battery Weight =	3.09 lbs	
		B * REP = 3.09
Manufacturing Cost Multiplier (MFHR)	C= \$ 20	
WBS 1.0 Wings		
Wing Span=	7 ft	*
Max Chord=	1.125 ft	*
# of Control Surfaces =	2	*
		WBS 1.0 = 71.0 hrs
WBS 2.0 Fuselage		
Fuselage Length =	5 ft	*
		WBS 2.0 = 50.0 hrs
WBS 3.0 Empenage		
# of Vertical Surfaces w/o cntrl =	0 v.s.	*
# of Vertical Surfaces w cntrl =	1 v.s.	*
# of Horizontal Surfaces w cntrl =	1 v.s.	*
		WBS 3.0 = 20.0 hrs
WBS 4.0 Flight Systems		
# of Servo or Motor cntrler =	5 ser	*
		WBS 4.0 = 25.0 hrs
WBS 5.0 Propulsion Systems		
# of engines	1 eng	*
# of propellers	1 prop	*
		WBS 5.0 = 10.0 hrs
		MFHR 176
		RAC 9.655

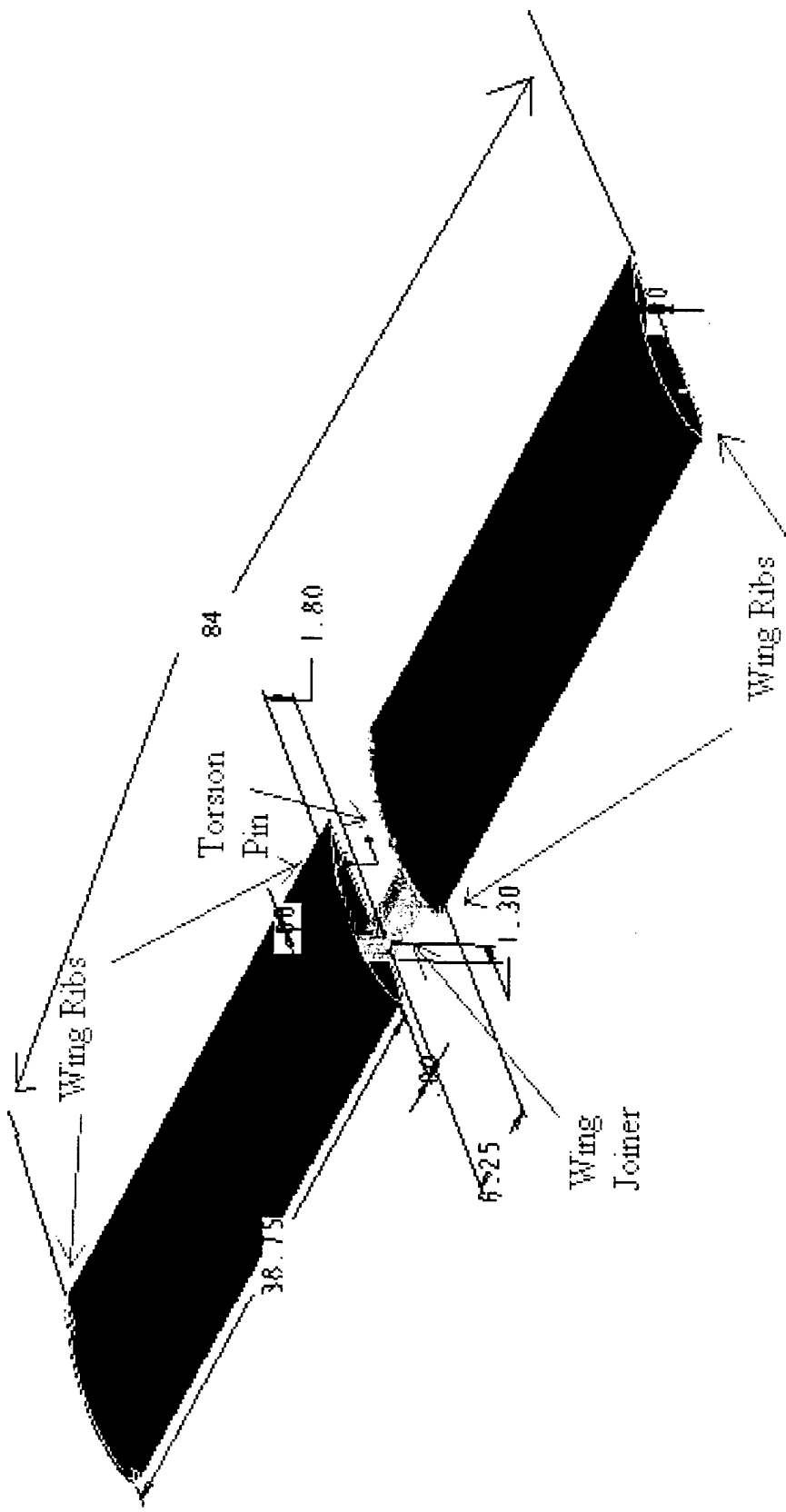
5.7 Drawings
5.7.1 Overall aircraft



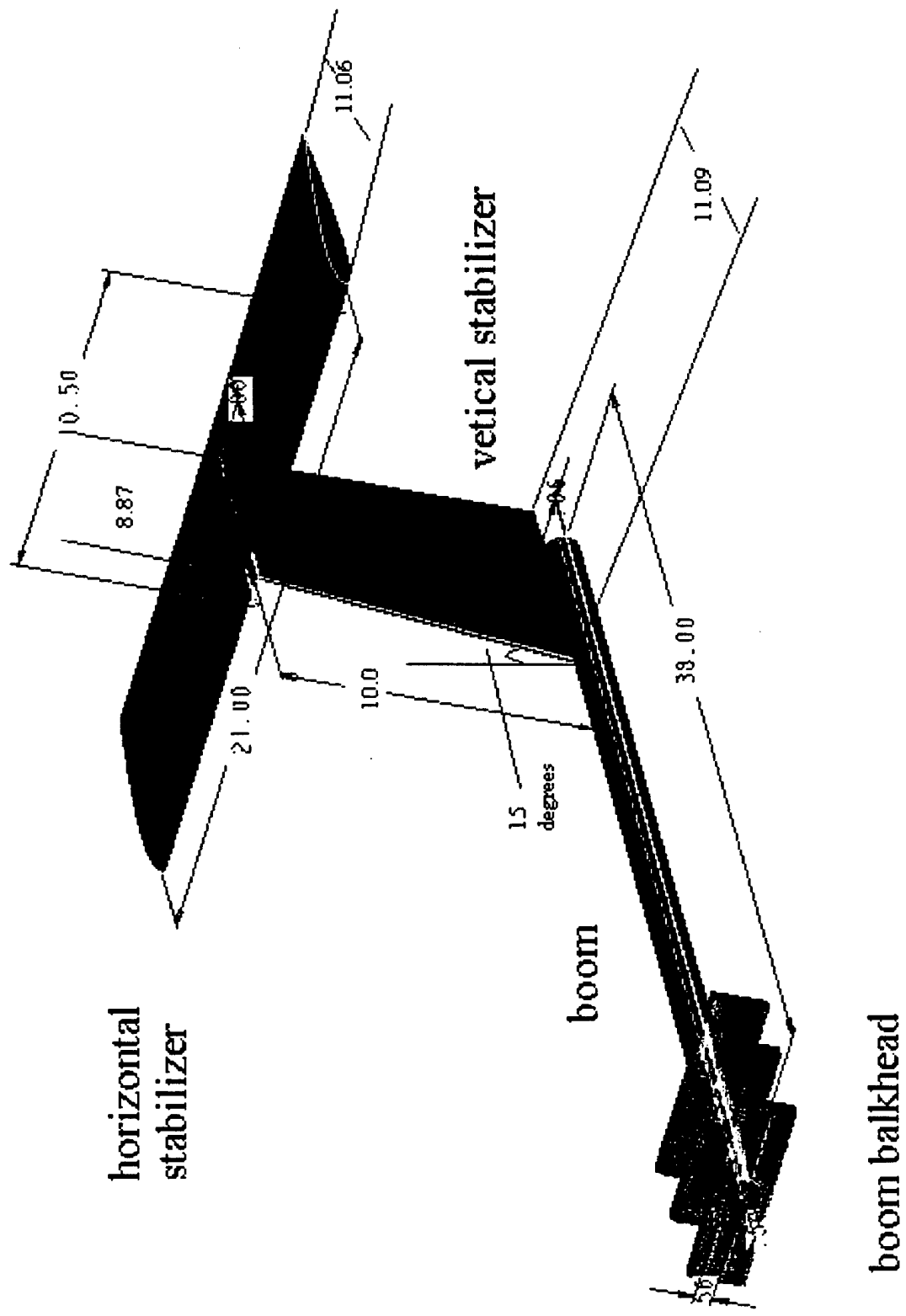
5.7.2 Fuselage Structure with Payload Deployment System



5.7.3 Dimensions of the Wing Assembly



6.7.4 Dimensions of the Tail



6 Manufacturing Plan and Techniques for Furious Flier

6.1 Manufacturing Processes and Feasibility

The necessary skills, tools, and materials needed to produce the Furious Flier (FF) this year were many. Manufacturing an aircraft predominantly of composite materials brought with it certain difficult yet unavoidable challenges. Some of these challenges included, but have not been limited to; ease of working with the materials, cost of these materials, experience or skills needed to work with these materials, the time involved in manufacturing component parts, reproducibility of these parts in both shape and strength, and having the necessary tools to work with these materials before, during and after they become components for our aircraft. Below is a Gantt Chart depicting the progress of the team (Fig. 6.1).

Design/Build/Fly Project 2002-2003

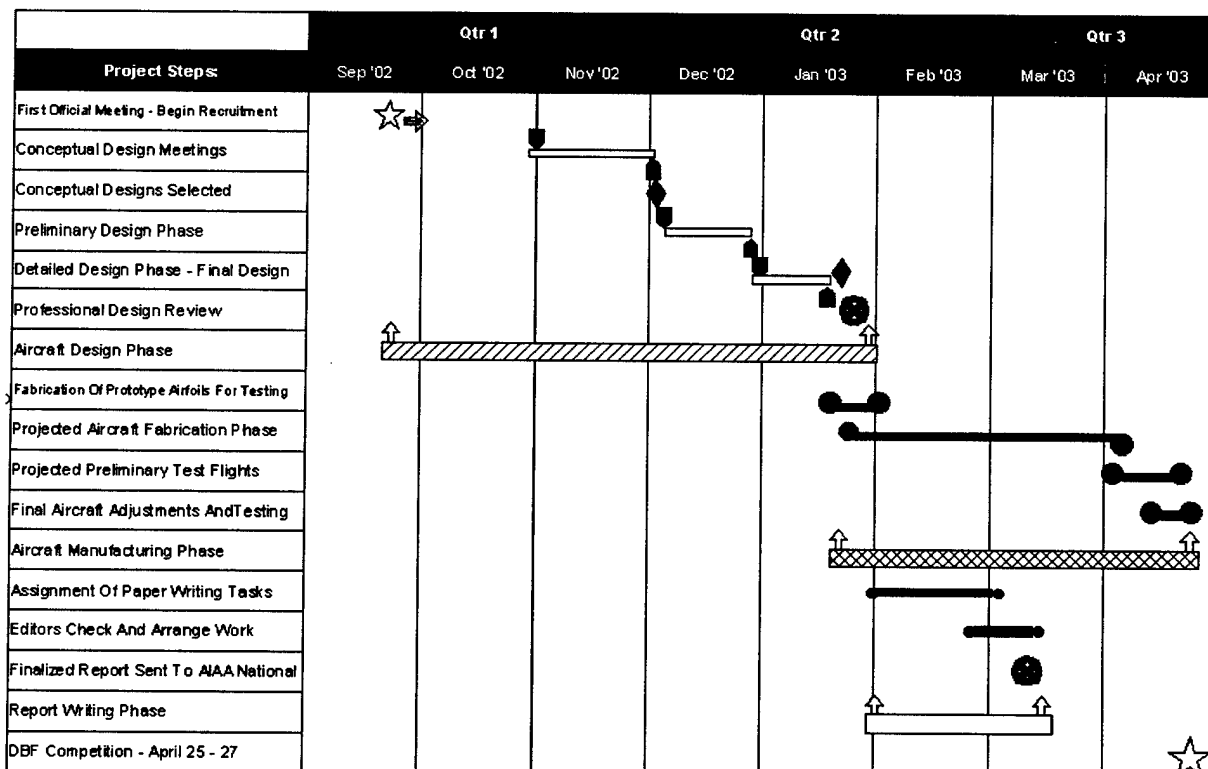


Figure 6.1: Gantt Chart

6.2 Manufacturing Processes by Aircraft Component

6.2.1 Manufacturing FF's Wings and Empennage

In order to create a wing structure that was strong yet light, we opted to construct a foam core that would be covered in a lightweight composite skin. To add structural strength to the wing, a spar (stringer) was inserted at its quarter cord. To create the wing's foam core, we used a data base of airfoils to get a set of (x,y) plane coordinates for our foil, the Selig 4022. Feeding these coordinates into a

computer program at school networked with a laser computer aided machining (Laser CAM) device, we were able to cut templates, or exact dimensioned replicas of our airfoil's cross section out of thin plywood. Attaching one of these templates on each end of large blocks of low-density white foam and using a hot wire (bow) cutter, we drew a heated wire over the wooden templates and were left with the foam cores of our wings. Very fine sand paper was then used to eliminate any waves or imperfections that may have resulted from the bow cutter, and to round the leading edge of the wing. Large pieces of fiberglass cloth were then cut and wetted with epoxy and laid onto the foam wing. Mylar, a thick but very smooth and pliable plastic, was then draped onto the wing and everything was placed onto a sealed bag which held a vacuum hose. Applying a vacuum to the bag (bagging/bagged) would eliminate the air inside and apply equal pressure to the core as it cured. The Mylar will give the skin of the wings a very smooth look and feel and will help to reduce drag during flight.

While the same hot wire process was used to cut out horizontal and vertical stabilizers for the aircraft, no spars were needed because the stabilizers are fairly small and the skins will acceptably take all of the loads encountered during flight. However, to err on the side of caution several strands of carbon tow were affixed to the leading and trailing edges of both of the stabilizers to ensure strength in flight and during transportation. Similarly to the main wing, the horizontal and vertical stabilizer foam cores were covered with a fiberglass skin and bagged to cure with Mylar to keep surfaces as smooth as possible.

6.2.2 The Spar and Spar Joiner Construction

The afore mentioned spar was made by first removing a section of the foam wing core 1 inch wide about the quarter cord length from the entire length of the wing. Using layers of epoxy wetted bidirectional carbon cloth, we placed six layers of the cloth (two each of three different lengths: one-third, two thirds, and full length) onto both the top and bottom of the excised piece of foam and bagged it overnight to cure. The inner third of the spar has been covered on each side by six layers of carbon cloth, the middle third by four, and the outer third by only two, in order to ensure enough wing strength to survive a 3 "G" load while keeping weight to a minimum. Excess carbon fibers were sanded off before proceeding to lay approximately 3 layers of epoxy wetted fiberglass cloth around the entire spar structure and bagging again.

At this point, we decided to test the strength of our spar by keeping four inches of the inner portion of the spar (root end) stationary in a bench vice and setting several small weights on the suspended end. We were disappointed to see a fair amount of deflection in the length of the spar after loading with less than 5 pounds. Had we continued with this design, the wings may have buckled during the "wingtip test" or worse, during flight. A stronger and stiffer design was needed for our spar application.

In our never-ending search for high strength with lightweight, we were turned to balsa wood to reconstruct the wing spar. Balsa, with its natural fiber structure and lightweight was as ideal for our application as we were going to find. A piece of balsa was trimmed to the exact dimensions of the now

broken foam core of our previous spar. We then subjected the wood the same rigorous layers of unidirectional carbon fibers, wraps of fiberglass, and finally two extra layers of unidirectional carbon on the three and a half inches of the spar nearest its root. After completely curing, we tested the new spar in the same fashion we had the last. With almost 10 pounds of weight near the spar's tip, there was very little deflection and the spar was deemed acceptable. Another balsa spar was made as described above for the other wing and the spars were then replaced and bonded into their respective wings. These processes made a sufficiently light yet very strong box-beam structure central to the wing helping to keep it rigid under all conditions.

The spar joiner was an engineering challenge from the start. All loads on the wings will be transferred through this joiner, necessitating that it be stout. While most machined metal joiners would have been sufficient strength wise, their weight was unacceptable. Our attention turned to carbon once again and a mold was made of aluminum to the exact dimension of where our joiner would sit when placed into the fuselage. The spars were temporarily attached together and placed into the mold. Epoxy wetted unidirectional carbon strands were then placed on all sides of the spar until the two sides and the top and bottom had equal amounts of carbon material between the spar and the mold. The mold was then closed and left to cure, making an exact female acceptor for the spars to slide into during assembly. Upon curing, the spars were removed from the joiner, and the joiner removed from the mold. The joiner was then sanded into the exact shape needed for its installation into the fuselage.

6.2.3 Fuselage Construction

Due to this year's different and fairly unique set of requirements, the fuselage took on a shape that directly resembled its payload, a box. While it is not the most aerodynamic of choices, it was necessary in order to comply with the "packing box" constraints. With exception of the plane's nose cone and main fuselage floor, the fuselage is made entirely of composite "sandwich material" which has proven to be strong and light in previous years' contests. Slices one-fourth inch thick of high-density "blue" foam were cut from larger blocks. These slices were then sandwiched by a layer each of epoxy wetted unidirectional and bidirectional carbon cloth on top and bottom, then vacuumed. After curing, marks were made on the material and panels were cut in the exact dimensions of fuselage secondary floors, walls, and fairings. The primary floor of the fuselage was produced from a one-fourth inch thick piece of aircraft grade birch plywood. This was necessary in order to have a very stiff, load and vibration absorbing central backbone of the aircraft. Although it was slightly heavier than the sandwich material, the extra strength it gained was well worth it.

The nose cone of the aircraft is a fiberglass shell with an internal rib structure of balsa wood that will act as a bulkhead for the motor. By cutting and sanding the blue foam to a desired shape made a male foam mold of the nose cone. The mold was then covered with four layers of epoxy wetted fiberglass and bagged until cured. The foam mold was then removed from its shell and internal measurements were taken. Using these measurements, ribs of balsa wood were cut out and placed in the nose cone

forward of the motor mount on the fuselage to act as bulkheads for the motor. A small hole was cut at the front of the nose cone for the propeller shaft to pass through and as a ventilation hole for motor cooling.

6.2.4 Boom

The boom attaching the fuselage body of the plane to the empennage is a pre-manufactured carbon composite spun tube with a one inch inner diameter. The tail section is attached to the boom with two nylon screws threaded through the boom from the bottom and into the vertical stabilizer. The boom attaches to the fuselage through three bulkheads internal of the body. There will be a notch on the boom that will allow the entire tail section to be locked into place when the boom turned a quarter of a revolution about its axis.

6.2.5 Landing Gear Manufacturing

The landing gear for the aircraft was made with prepreg carbon composite. A mold for our landing gear was made by rolling a sheet of aluminum that had been machined to the desired shape and curve of the gear. The carbon was then laid onto the machined piece and placed in an autoclave for curing. When the gear emerged, a hole was drilled at the bottom for the wheel axles, and at the top several holes were made in order to attach the gear to our fuselage.

6.3 Costs, Skills, and Schedules

6.3.1 Cost of Composite Materials

While the cost associated with using composite materials is greater than using non-composites the decrease in weight and increase in strength made composites the hands down choice for many manufacturing applications. From the start of the project, the team anticipated incurring the cost of these materials and therefore was budgeted for their purchase. Nonetheless, care was taken in purchasing materials like carbon cloth, fiberglass, and epoxies to reduce cost and waste.

6.3.2 Skills and Tools Needed to Work with Composites

Nearly half of this year's team is returning members from last year's team. This helped to create a group of students that were familiar with working on composite materials. This knowledge included not only the ability to manipulate these materials in the necessary fashion, but also being able and confident to use the tools associated with building composites such as sanders, heat guns, vacuum pumps, and rotary tools. Using epoxy resins is also a small science of its own in which attention to detail is essential. Of course safety is always a priority, so goggles, face masks, gloves, breathing filters and lab coats were supplied to those working in and around the shop to protect them from any lab associated dangers.

6.3.3 Manufacturing Schedule

Manufacturing began as soon as funds became available to purchase needed materials and tools. The team met Thursdays, Fridays and Saturdays in order to get 12 to 15 hours of work completed

each week for the first 4 weeks of the manufacturing phase. Goals were set for what needed to be completed by the end of each week in order to keep the team organized and motivated. At least 2 team members met to do construction at any given time. One "veteran" team member was present whenever any manufacturing was taking place to ensure safety, productivity and quality. The Furious Flier is planned to be fully completed by the last week of March 2003. Completing the manufacturing several weeks before the competition will enable the team to have plenty of time in which to do flight testing and make any last minute changes or amendments to the aircraft. This will also enable our pilot to become accustomed to the plane and its characteristics before arrival at the competition site.

7.0 Test Planning

7.1 Dynamic Test: Graupner Motor

The purpose of testing the Graupner Ultra 3300/5 is to help in determining what RPM gives the greatest efficiency for the motor used. The motor in question is a Graupner Ultra 3300/5 and operates at 18 volts with a gear ratio of 2:1. Figure 7.1 is arranged to use two relationships to best confirm how the motor should be operated for best efficiency in flight. The first relationship is that of power (watts) and RPM. The second relationship is that of current (amperes) and efficiency.

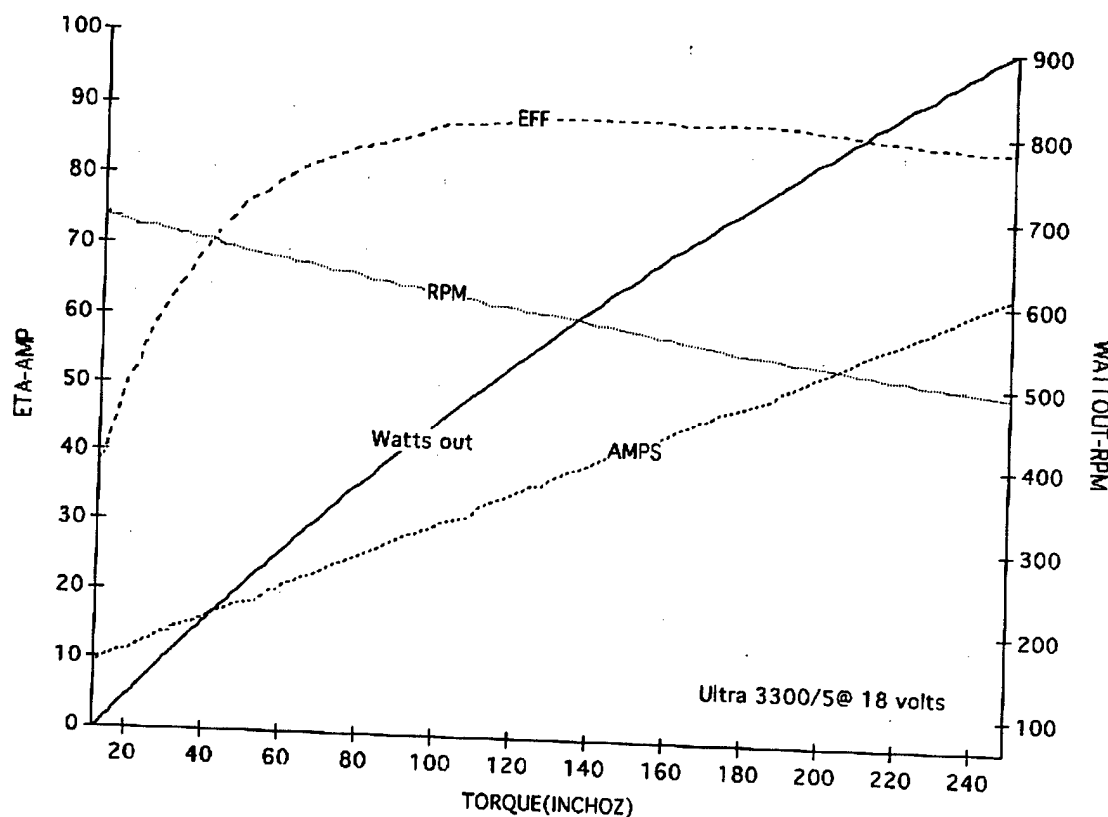


Figure 7.1: Dynamometer plot

An example of how the graph yields information is attained by examining the data for a specific efficiency. When the motor is performing at 60% efficiency, the current supplied to it is 15 amperes. At this efficiency the power from the motor is 8W. Also, the RPM exerted by the motor are 675.

The data on the graph indicates that the highest efficiency achievable by the motor is 89%. This occurs when the current supplied to the motor is 40 amperes. At 40 amperes, the power produced by the motor is 580. From this data it is determined that the RPM ideal for maximum efficiency is 560 RPM. Therefore the motor should ideally be operated at 560 RPM to achieve maximum efficiency.

The process of gathering the data represented in the graph took a total of one hour to complete by the UCSD D.B.F. team. The data serves to provide direction when deciding how the motor's performance should be integrated to the aircraft as a whole. For example, if it is not possible to operate the motor at 560 RPM during flight, the data represented in the graph will aid in choosing another suitable RPM setting for the aircraft's operation. One reason why the motor may not be able to be operated at 560 RPM during flight could be the interaction between the vibrations given off by the motor and the aircraft structure. In such a case the data in the graph would prove indispensable in deciding how the motor should be operated.

8.0 Reference:

1. Abbot I.H., Theory of Wing Sections, Dover Publications Inc, 1949.
2. Nelson, R., Flight Stability and Automatic Control, McGraw Hill, 1989.
3. Nicolia, L.M., Fundamentals of Aircraft Design, METS Inc, 1984.
4. Peery, D.P., Aircraft Structures, McGraw-Hill Inc., 1982.
5. Przemieniecki, J.S., Performance, Stability, Dynamics, and Control of Airplanes
6. Raymer, D.P., Aircraft Design: A Conceptual Approach, AIAA Education Series, 1989.

3 View Drawings

